

Review

Cytoskeletal Symmetry Breaking and Chirality: From Reconstituted Systems to Animal Development

Christian Pohl

Buchmann Institute for Molecular Life Sciences and Institute of Biochemistry II, School of Medicine, Goethe University, Max-von-Laue-Strasse 15, Frankfurt (Main) 60438, Germany;
E-Mail: pohl@em.uni-frankfurt.de; Tel.: +49-69-798-42589

Academic Editor: Albert K. Harris

Received: 31 July 2015 / Accepted: 4 November 2015 / Published: 11 November 2015

Abstract: Animal development relies on repeated symmetry breaking, e.g., during axial specification, gastrulation, nervous system lateralization, lumen formation, or organ coiling. It is crucial that asymmetry increases during these processes, since this will generate higher morphological and functional specialization. On one hand, cue-dependent symmetry breaking is used during these processes which is the consequence of developmental signaling. On the other hand, cells isolated from developing animals also undergo symmetry breaking in the absence of signaling cues. These spontaneously arising asymmetries are not well understood. However, an ever growing body of evidence suggests that these asymmetries can originate from spontaneous symmetry breaking and self-organization of molecular assemblies into polarized entities on mesoscopic scales. Recent discoveries will be highlighted and it will be discussed how actomyosin and microtubule networks serve as common biomechanical systems with inherent abilities to drive spontaneous symmetry breaking.

Keywords: actin; myosin; microtubules; polarity; embryogenesis; chirality; symmetry breaking; *C. elegans*; drosophila; actin; myosin; spindle; cell division

1. Introduction

Symmetry breaking in biological systems is a pivotal phenomenon that has fascinated both biologists and researchers of other disciplines for decades [1]. The discovery of signaling pathways underlying symmetry breaking by inductive cues has led to great efforts in identifying the responsible signaling centers and molecules that constitute the cue. Several models have been proposed that unify the functions

of signaling pathways in different organisms [2–5]. In parallel, our understanding of symmetry breaking in biological systems has also grown substantially in the recent past. In many cases, causal relationships between inductive cue and biophysical outcome have been demonstrated (Table 1). It has even been possible to rewire existing biological systems that undergo symmetry breaking in a way that competing polarities can be generated [6].

Independently of the specific developmental process, metazoa seem to use a remarkably conserved molecular toolset for cue-dependent symmetry breaking including actomyosin and microtubule networks, the PAR genes, Wnt and Notch signaling [7–10]; differential deployment and the vast number of accessory factors ensure that this toolset can generate drastically different species-specific outcomes on a macroscopic scale.

Table 1. Examples for symmetry breaking processes in animal development for which both polarizing cue and biophysical mechanism are known.

System	Polarizing Cue	Physical Effect	Effector Molecule	Developmental Outcome
<i>S. cerevisiae</i>	Cdc42 activation	transport of Cdc42 to plasma membrane	F-actin	polar cap formation followed by budding [11,12]
<i>C. elegans</i>	Sperm entry	A/P polarized cortical actomyosin flows	cortical actomyosin	A/P symmetry breaking by segregation of PAR domains [13–16]
<i>D. melanogaster</i>	Toll	planar polarized actomyosin contractility	non-muscle myosin II	convergent extension during gastrulation [17]
<i>Danio rerio</i>	fluctuating adhesion, myosin contraction at cell rear	large-scale actin network disassembly by myosin II	cortical actomyosin	symmetry breaking and polarized migration [18]
<i>Mus musculus</i>	non-canonical Wnt signaling	posterior tilt of nodal cilia	nodal cilia	L/R symmetry breaking by asymmetric nodal flow [19,20]

In contrast to cue-dependent symmetry breaking, spontaneous symmetry breaking relies on inherent instabilities which endow cellular systems with the ability to couple a metastable state to a non-spontaneous event (e.g., a developmental signal), thereby generating a new state or pattern [21]. A well-studied example for spontaneous symmetry breaking is the emergence of chirality during development. Here, many different and often organism-specific mechanisms and molecules have been described. Such diversity notwithstanding, it seems that anisotropies at the level of the microtubule and actomyosin cytoskeleton represent a common biophysical principle underlying spontaneous symmetry breaking.

While symmetry breaking in physics implies a transition from a homogenous to a patterned state, a superficially homogenous structure in a biological system often already contains imperfections and thus seeds of asymmetry. This might be one reason why it has been challenging to elucidate the mechanisms of spontaneous symmetry breaking in development since capturing the precise state and configuration of a biological systems is much more difficult than in a reconstituted physical, chemical or biophysical systems. Notably, recent breakthroughs further strengthen this notion: The generation of organoids *in vitro* has revealed that systems originating from a few different cell types (derived from stem cells or organ

progenitors) can self-organize into structures that resemble to their *in vivo* counterparts. Organoids recapitulate cell sorting, spatially restricted lineage commitment and pattern formation [22]. Hence, complex developmental processes can apparently take place independently of developmental history or topology, and, thus, most likely also without some of the intricate cue-dependent symmetry breaking phenomena identified previously. It is therefore essential to better understand emergent phenomena such as collective cell shape changes, establishment of gene expression domains and signaling centers in the context of inherent metastabilities of biological systems.

In this review, recent advances achieved by utilizing *in vitro* and single cell systems to better understand the molecular and biophysical origins of spontaneous symmetry breaking will be discussed. Further, how these discoveries relate to findings in developmental biology will be explained. Finally, several discoveries that broaden our understanding of cue-dependent symmetry breaking *in vivo* will be highlighted with a focus on examples that use the same biophysical principles as discussed for spontaneous symmetry breaking.

2. Spontaneous Symmetry Breaking *in Vitro* and in Single Cells

For animal development to proceed, it is important that a biological system initially is in an intrinsically metastable state so that symmetry breaking can occur. Metastability ensures that an energy barrier has to be overcome which is higher than the inherent energetic fluctuations (noise) of the system [21]. Metastability has been particularly well described on the level of morphogens [23] and on the level of transcriptional networks, leading to cell differentiation, and overcoming earlier concepts of hierarchical cell fates [24]. For developing biological systems, biomechanical metastability at the level of the cytoskeleton is equally important. The two major bio-architectural elements in this context are microtubule-motor systems and actomyosin networks.

As symmetry breaking *in vivo* involves protein-protein interaction networks [25,26], it is difficult to reconstitute such a process *in vitro*. Nevertheless, reductionist *in vitro* systems based on purified proteins frequently supplemented with cell extracts can be highly valuable to better understand how individual components contribute to a complex process. Also, they help in identifying common emergent properties of systems that show spontaneous symmetry breaking.

2.1. Microtubules and Microtubule-Motor Systems *in Vitro*

Microtubules are comprised of α/β -tubulin dimers polymerized in 13 parallel, staggered proto-filaments which associate laterally and close on themselves, thereby forming a hollow tube. The contacts in the tube are homotypic in that α - α and β - β contacts are formed with the exception of heterotypic contacts (α - β) at the seam where the protofilament lattice has closed to form the hollow tube (Figure 1a). Polymerization takes place when tubulin is bound to guanosine tri-phosphate (GTP) (usually at the (+)-end), while de-polymerization is favored when GTP is hydrolyzed to guanosine di-phosphate (GDP) (at the (–)-end) (Figure 1a). Seminal experiments by Mitchison and Kirschner have demonstrated that microtubules show the striking intrinsic property of dynamic instability, meaning that growing and shrinking microtubules can co-exist in the same system [27,28]. Additionally, microtubule de-polymerization can also occur stochastically in a catastrophic process [29]. This has been explained phenomenologically by microtubules being stabilized by a cap of tubulin-GTP, which when lost, triggers de-polymerization

catastrophe [30]. Several models have been generated to account for these instabilities [31–37]. Furthermore, the term “structural plasticity” has been introduced to describe additional changes in filament/polymer structure without change(s) in the chemical state of its bound nucleotide [38]. The conceptual difference to older models being that microtubule dynamics observed *in vivo* are more complex than simple polymerization/de-polymerization models would predict. For instance, de-polymerizing ends are curling while stable ends are straight, the latter has been explained to depend on a conformational change after GTP binding that straightens the α/β -tubulin dimer to favor lateral contacts [39]. These conformational changes not only contribute to the intrinsic polymerization dynamics of microtubules but also seem crucial for microtubule-associated proteins to monitor, control, build, and modify microtubule networks [40]. Most recently, it was shown that structural plasticity is key to the modulation of microtubule dynamics by (+)-end-binding proteins since they recognize a structural state rather than a chemical state and promote compaction of the microtubule lattice, thereby facilitating GTP hydrolysis [41].

These intrinsically non-linear properties have made microtubule preparations an attractive *in vitro* model for the study of dissipative processes, e.g., to understand oscillations [42,43], symmetry breaking [44], and self-organized formation of spatial patterns in the form of traveling waves and polygonal networks [45]. Notably, these behaviors can be attributed to the fact that dense solutions of rod-shaped polymers generally tend to behave like nematic liquid crystals [46].

Concerning the forces that drive spontaneous symmetry breaking in dense microtubule solutions *in vitro*, it has been discussed that a gravitational field can apparently be sufficient *in vitro* [47], which has fueled the idea that gravitational force might also contribute to microtubule self-organization and therefore symmetry breaking in cellular systems [48]. It has been proposed that such *in vitro* patterning of microtubule solutions by gravity is most likely due to (1) interactions between microtubules through tubulin concentration gradients if microtubules are separated by a distance less than the diffusion growth length (meaning very high concentrations); (2) constant turnover at microtubule ends; and (3) so-called “avalanche-like correlated clusters” or longer microtubule fragments generated by dynamic instability that can re-associate with neighboring microtubules [49]. The latter effect will lead to far-from equilibrium kinetics and spatially correlated dynamics at the macroscopic level most likely due to the liquid crystal-like properties of such dense solutions. It should be pointed out that these gravity-dependent phenomena are restricted to non-physiologically dense *in vitro* preparations and their *in vivo* relevance is controversial [50–52], especially since forces generated in microtubule assemblies are orders of magnitude greater than those generated by gravity. However, independent of the forces needed to organize microtubules into liquid crystal-like states, there is recent bona fide evidence of liquid crystal-like behavior of microtubules in cells [53,54].

More than 25 years ago it has been proposed that fluid motion in rod-containing solutions might not be continuous but organized in small domains and what has been called gelation in such systems might simply represent liquid crystal domain formation [46]. To be endowed with liquid crystalline-like self-organizing potential, such microtubule systems need motor proteins. The two main microtubule motors are kinesins and dyneins [55]. They exhibit specific end-directed motor activity either *versus* the (+)-end (many kinesins) or the (–)-end (dyneins and several kinesins) (Figure 1b). Capitalizing on the liquid crystal-like properties of microtubule-motor *in vitro* systems, different bio-mimicking systems have been designed that either exhibit polar or nematic symmetries. The former systems show liquid

crystal defects in the form of asters and vortices (Figure 1d), the latter so-called disclination defects (Figure 1c, right). Leibler and co-workers conceived the polar system that forms dynamic crosslinks between adjacent microtubules through tetrameric kinesin motors [56,57].

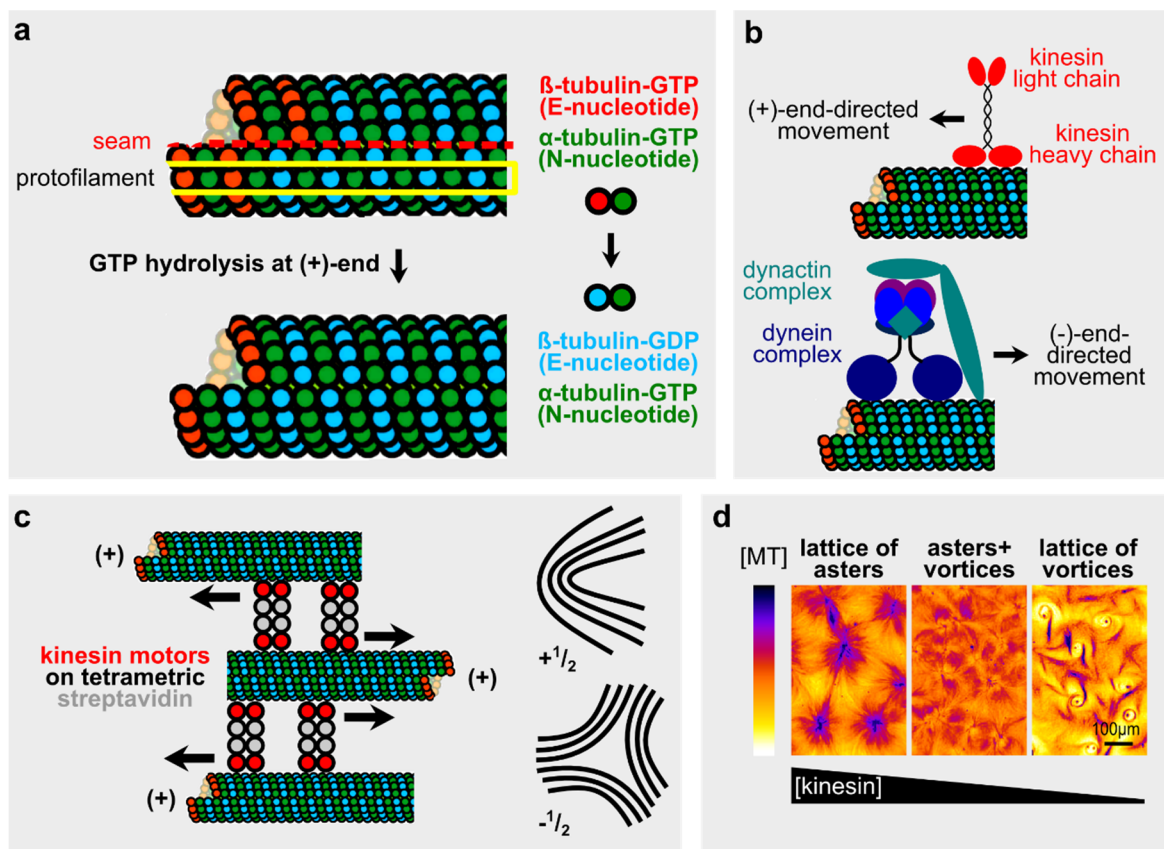


Figure 1. Microtubule organization, motors and properties of microtubule-motor systems. (a) Microtubule structure and polarity. Note the difference in the size of the guanosine tri-phosphate (GTP)-cap after hydrolysis. This will lead to de-stabilization of the (+)-end. Microtubule model adapted from [58]; (b) Microtubule motors and their polarity. Models adapted from [59] (c) Left: Behavior of the reconstituted system used in [60,61]. Note the extensile behavior of the system with microtubules of opposite polarity moving in opposite directions; Right: Disclination defects observed in these systems; (d) Different concentrations of the motor (kinesin) in microtubule-motor reconstituted systems [56,57] leads to different outcomes. False-colored experimental outcomes adapted from [56].

In this system, asters that resemble monopolar mitotic spindles are formed when the system is confined in a nearly two-dimensional space. However, asters in round confinement are not stable and transit into vortex structures. Without confinement, this system can either develop into a lattice of vortices (at low kinesin concentration), a lattice of asters (at higher kinesin concentrations) [56], or into a network of poles that are connected by aligned microtubules (when both a (-)- and (+)-end-directed motor are used) [57] (Figure 1d). The type of network formed is determined by the relative amount and ratio of motors as well as their residence time on microtubule ends. Notably, the vortex-type of self-organization has been investigated in more detail recently [62]. Analyzing the microtubule alignment process necessary to form a vortex, the authors find that a direct collision of microtubules is followed by bending. Reptation

or snake-like slithering in smooth trajectories will eventually lead to mesoscopic self-organization. These characteristics can also give rise to long persistent lengths required for formation of vortices spanning ~400 micrometers [62].

Further modifying the original system by Leibler and co-workers (Figure 1c), the Dogic and Bausch laboratories have recently described experiments using microtubules-motor systems that assemble into differently dynamically behaving, self-organized structures. They exhibit chaotic flow and autonomous motility [60], thereby reflecting *in vivo* phenomena like cytoplasmic streaming [63] or microtubule arrays in plant cells [64], respectively. Importantly, also here self-organization relies on microtubule collisions and alignment after collisions. However, in this system, polarity sorting is observed after collisions leading to the formation of a nematic material that are mostly (if not exclusively) extensile on mesoscopic scales (Figure 1c, arrows). This is in stark contrast to reconstituted actomyosin systems that usually exhibit contractile behavior. If the microtubule-motor system is assembled as active nematic vesicles, it can even change its shape with streaming filopodia-like protrusions [61]. This is the result of topological defects (disclinations) that are caused by spherical confinement (Figure 1c, right). Furthermore, when the same reductionist system is assembled on a surface, it can exhibit beating patterns that resemble those of cilia [65]. Although not organized into cross-linked microtubule doublets as in cilia, elastic microtubule bundles can spontaneously synchronize their activity to produce collective behavior similar to waves observed in ciliary fields [65].

Taken together, minimal microtubule-motor systems—with far from equilibrium kinetics—are able to recapitulate basic collective phenomena that are most likely also occurring during developmental symmetry breaking. These include nematic liquid crystal-like behavior with polar or nematic polarities, self-organization into macroscopic dissipative structures, and chirality (as far as vortex structures are concerned).

2.2. Microtubules in Neuronal Polarity and Spontaneous Phenomena during Cell Division

Although microtubules fulfill central functions during asymmetric cell division, they are usually not the structural element where symmetry is broken first. This seems to be due to microtubules usually not constituting a boundary element of animal cells that directly regulates cell shape. Therefore, they play a less prominent role in spontaneous symmetry breaking than actomyosin networks as will be discussed in detail below. Notwithstanding these differences between cytoskeletal systems, the role microtubules play during establishment of polarity in neurons will be highlighted using two examples where alterations of microtubule organization leads to spontaneous symmetry breaking during cell division.

Neurons *in vitro* represent a system with elaborate broken symmetry on a single cell level and intrinsic polarity without external cues. In this symmetric *in vitro* environment, neurons grow multiple processes or neurites from which only one will form the axon [66–68]. This is the neurite with the growth cone of lower actin density and highest actin turnover [69]. The other processes later become dendrites. It has become clear that axon specification requires both a complex interplay between microtubule ends and cortical actin [70,71] strongly dependent on microtubule ends undergoing simultaneous reorganization via dynamic instability [72]. Initially, it was suggested that after stochastic entry into the axon, selective stabilization of microtubules occurs either by a spatial or temporal gradient of microtubule dynamics or by cortical capture of dynamic microtubule ends. This would then contribute to symmetry breaking

during axon specification [73] (and references therein). However, it has now been demonstrated that microtubules will accumulate in the longer process most likely without any selective stabilization, confirming that symmetry breaking at the level of cell shape (in this case deploying actomyosin) directs axon specification [73]. These findings also explain why axonal polarity is established over hours/days and not in minutes, since both length-dependent axon selection and restriction of the activity of the polarizing machinery to one growth cone are both very slow processes. Specifically, polarization of the axonal growth cone involves the interaction of conserved polarity regulators (the Par3/Par6/aPKC complex) with axonal microtubules. This complex consists of two PDZ domain-containing proteins (Par3 and Par6, which engage in multiple protein-protein interactions, see Figure 2a) as well as an atypical protein kinase C (aPKC) [26,74,75]. The complex is initially localized at all neurites' growth cones but then becomes restricted to the axon due to positive feedback [76]. Here, Par3 directly regulates microtubules by binding, bundling and stabilizing them with its N-terminal part, which is intra-molecularly suppressed by its C-terminal part [77]. These activities are crucial for axonal polarization and could reflect some of the properties that have been observed in *in vitro* systems, where emergent phenomena also rely on high local concentrations and nematic-like ordering.

In sum, it seems that spontaneous symmetry breaking in neuronal growth cones by alterations in actomyosin dynamics leads to transient lengthening of a neurite, which through positive feedback on the level of microtubule end capture and stabilization by gradual enrichment of the Par3/Par6/aPKC complex allows the system to stochastically switch from a metastable into a stable state with broken symmetry. Interestingly, the polarity system used here to reinforce the asymmetric state acquired through a stochastic process can also operate on much smaller time scales (few minutes) in the case of embryonic polarization processes that are induced and not stochastic.

A quite different example where interactions of microtubules with the actomyosin cortical network can exhibit spontaneous symmetry breaking is during monopolar cell division: Here, an initially radially symmetric cell simultaneously polarizes both microtubules and the cell cortex as well as concentrates components of the cytokinetic furrow into a cap at one side of the cell [78]. This scenario can be generated by first inhibiting kinesin-5 which is responsible for generating a bipolar spindle, and then forcing them into cytokinesis by inhibiting the kinases Cdk1 or Mps1. Similar to the positive feedback between actomyosin symmetry breaking and microtubule enrichment in axons, it has been proposed that feedback loops between cell division furrow components and microtubules promote symmetry breaking during monopolar cytokinesis [78] (Figure 2b).

Less polarized spontaneous symmetry breaking that relies on coupling of cortical actomyosin dynamics to the microtubule cytoskeleton during cell division has also been observed when unnaturally long astral microtubules are generated by depletion of the microtubule depolymerizing mitotic centromere-associated kinesin (MCAK) [79]. Under these conditions, longitudinal spindle oscillations were observed after anaphase which were driven by non-muscle myosin II oscillations between polar cortices that probably became weakened before by excessive contacts to microtubules (Figure 2c). This suggests that under these specific conditions, microtubules can initiate spontaneous symmetry breaking similar to partial polarization by microtubule dynamics in developing embryos when actomyosin activity is compromised [80].

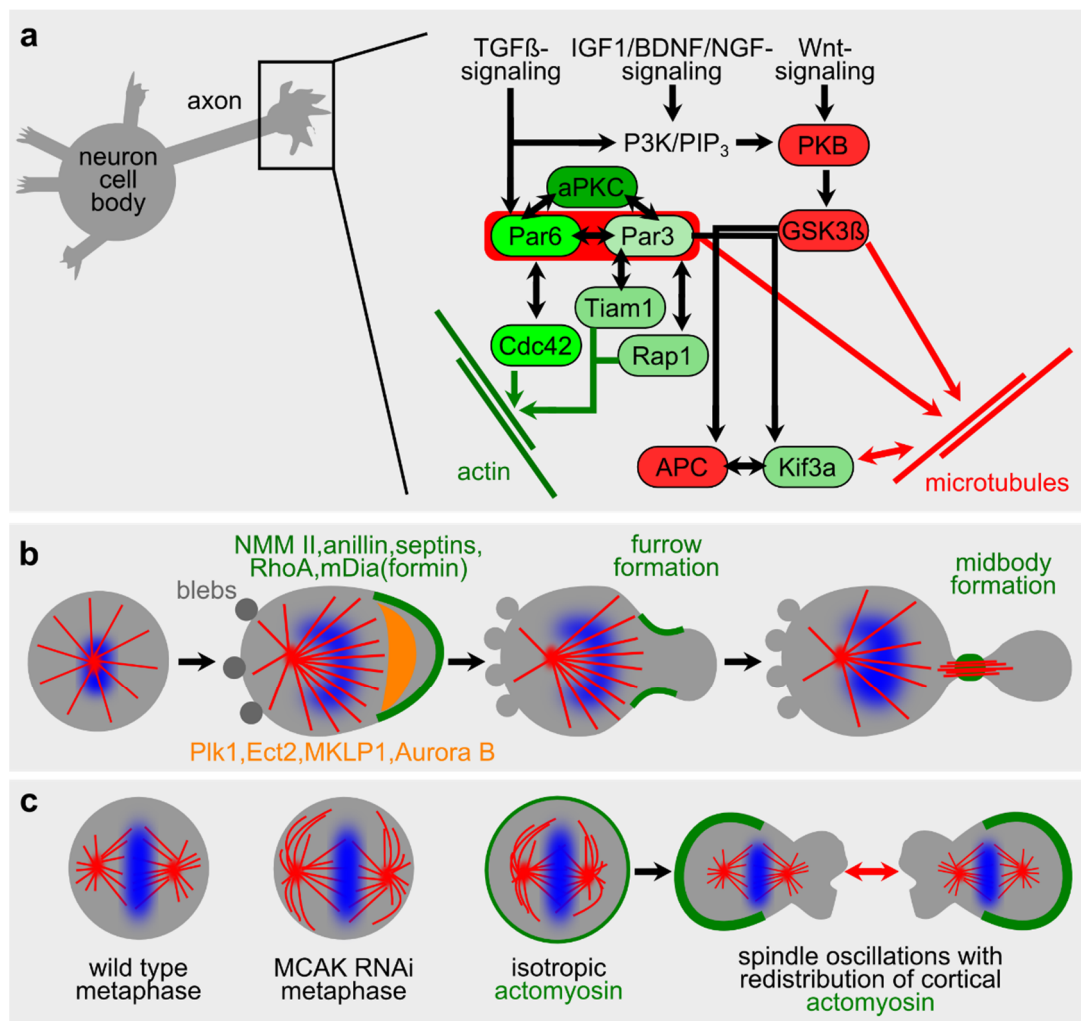


Figure 2. Microtubules in neuronal symmetry breaking and spontaneous symmetry breaking during mitosis. **(a)** Network of proteins centered around the atypical protein kinase C (aPKC)/Par3/Par6 complex. Direct interactions and activation are indicated by double arrows. Activities on actin dynamics are shown in green, activities on microtubule dynamics in red. Note that Par3/Par6 can directly interact with microtubules. Schematic adapted from [81]; **(b)** Spontaneous polarization of cleavage furrow components (green) and midzone components (orange) during forced exit of mitosis of cells with monopolar spindles. Note the continuous blebbing starting during anaphase. Red = microtubules; blue = chromatin. Schematic adapted from [78]; **(c)** Left: Differences in astral microtubule organization compared to wild type mitotic cells after depletion of the kinesin MCAK [79]. Spontaneous oscillations following anaphase onset. Note the re-polarization of cortical actomyosin during oscillation. Coloring as in panel (b). For high-resolution dynamics of oscillations, visit the supplemental material of [79] (time-lapse video microscopy data).

2.3. Actomyosin *in Vitro*

Attached to the inner face of the plasma membrane is the cortex, which gives cells their shape and allows them to polarize, divide, and move [82–84]. The main constituents of the cortex are actin filaments, non-muscle myosin II motors and various actin-binding, -cross-linking and -nucleating factors. These

factors form a hydrated network ranging from 0.1 to 1 μm in thickness. Key parameters that indicate how this network behaves biophysically are its degree of crosslinking, the ratio of branched to unbranched actin filaments, the amount of force-generating motors that create tension, and the strength of cortex-plasma membrane linkages. Tension in this molecular network can lead to multiple outcomes [21]: (1) If tension can relax through stochastic network breakage, this will lead to formation of blebs (Figure 3a), thereby releasing elastic energy. It will lead to actomyosin-membrane detachment and formation of a membrane protrusion (if the hydrostatic pressure in the model system is high enough) and constriction of actomyosin at distal sites in the network; (2) In contrast to blebbing, which is a singular elastic relaxation, continued contraction and relaxation accompanied by turnover of network constituents can lead to long-range rearrangements that reveal fluid-like properties for actomyosin networks [85]. In case of long-range coordination of contraction and expansion mesoscopic flows can be generated. This type of actomyosin flow-generating dissipative system is crucial for many morphogenetic processes in developing animals which will be discussed later [86]. Biophysical models of actomyosin based on hydrodynamic theory of active gels can explain flow-like dynamics by focusing on viscoelasticity and liquid crystal-like properties of the system [87,88].

Using starting conditions that were inspired by two very differently organized cortical actomyosin networks, the red blood cell's cortex with short filaments integrated into a loose network with a low degree of crosslinking and the outer hair cell's cortex with long-range filament order and a high degree of crosslinking, Dalhaimer *et al.* explored possible transitions and behaviors of these actomyosin networks [89]. In addition to the already discussed nematic liquid crystal-like properties of filamentous systems, crosslinkers can introduce elasticity into systems behaviors [90]. Based on simulations, it could be shown that while loose networks only resemble nematic liquid crystal-like fluids when under compression or shear, tight actomyosin networks like that of outer hair cells generally show this type of mesoscopic organization. Thus, systems properties do not simply rely on the relative concentration and filament length but also on intrinsic and extrinsic mechanical forces as well as additional factors that modulate filament polarity and organization.

To better understand how changes in systems properties affect biophysical dynamics of actomyosin, reconstituted systems have been developed that usually recapitulate actin polymerization on a surface and where additional molecules like cross-linkers or motor proteins can be added [91,92]. Consistent with the behavior of an active nematic fluid, collective motion (density waves, swirls) of actin filaments with directional persistence has been demonstrated when these interact with immobilized myosin in a high-density motility assay with planar geometry [93], thus in similar confinement as the self-organizing microtubule arrays discussed above. Another similarity to microtubule-motor systems at high densities is that cooperativity between interacting filaments together with weak alignment interactions generates these collective, mesoscopic phenomena. Hence, filament sorting is an important feature for these systems to develop liquid crystal-like properties and sorting can either lead to overall contractile (actomyosin) or extensible (microtubule-motor systems) dissipative structures. It seems likely that collective motion observed in planar confined reconstituted actomyosin systems represents density waves and therefore *in vivo* correlates of the dynamics observed during cortical flow.

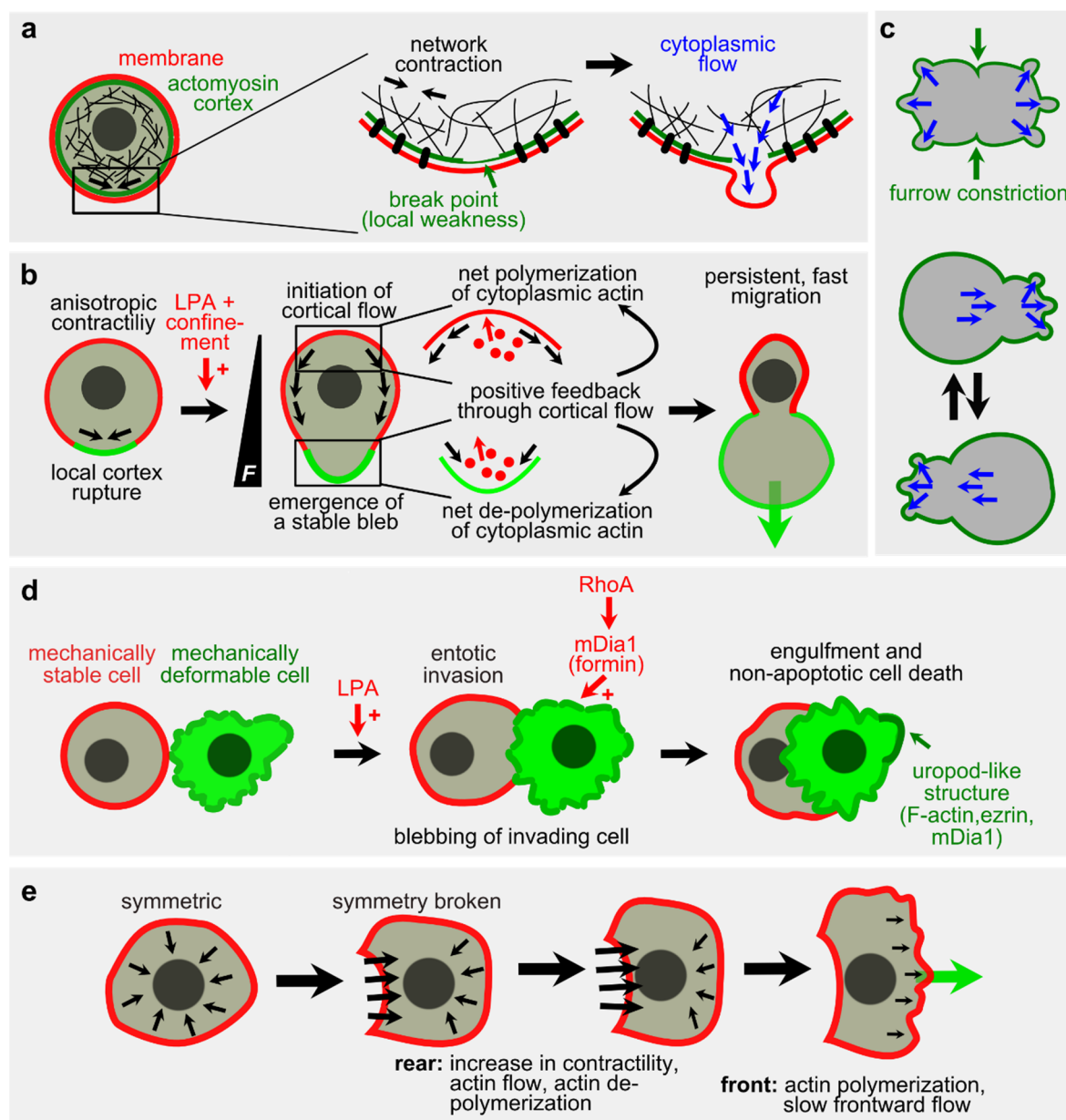


Figure 3. Spontaneous cellular symmetry breaking by blebbing and rear contraction. (a) Bleb formation. Schematic according to [94]. See text for details; (b) Spontaneous symmetry breaking by blebbing and persistent migration; adapted from [18]. Small black arrows show actomyosin cortical contractile flow. F = contractile force; red dots = monomeric actin. The green arrow indicates the direction of migration; (c) Top: Polar blebbing releases tensile stress and ensures symmetric ingression of the furrow (green arrows). Bottom: If a high pressure difference exists between the poles, shape fluctuations can occur that might lead to cytokinesis failure. Schematic adapted from [95]; (d) Asymmetric mechanical properties and blebbing of the invading cell contribute to entosis; see [96]; (e) Spontaneous symmetry breaking through rear contractility and forward-directed actomyosin flow can initiate cell migration; adapted from [97]. The small black arrows indicate tension force, the green arrow indicates the direction of migration. See also [98] and text for details.

Moreover, in a reconstituted system with planar geometry but inverse topology (where actin is bound to a membrane and myosin is added), actin turnover can be mediated by myofilament-driven actin fragmentation [99]. The latter findings and the tunability of physical parameters of actin networks by small changes in cross-linker concentrations [87] might explain how contractile networks can undergo fast remodeling *in vivo*. This is also consistent with the interpretation from the Sykes laboratory that symmetry breaking in reconstituted systems can be attributed to rupture of spherical actin networks when cortical tension surpasses a certain threshold [100]. The threshold is determined by a concentration window of capping protein that limits growth of branched networks nucleated by the Arp2/3 complex, and by a sufficient number of motors that pull on actin filaments [101]. Importantly, all these different molecular origins of spontaneous symmetry breaking *in vitro* (1) changes in contractility; (2) changes in cross-linker concentrations; (3) local changes in the rate of actin polymerization; and (4) different forms of actin polymerization (switches between unbranched and branched networks) have been found to either drive symmetry breaking *in vivo* or to remodel actomyosin networks in order to amplify broken symmetry from the cellular to the tissue, organ or organism level [84].

Besides reconstituted systems with planar geometries, one of the first systems where spontaneous symmetry breaking *in vitro* can trigger biological phenomena like cell motility was a system of beads coated uniformly with *Listeria monocytogenes* ActA that catalyzes actin polymerization [102]. In these experiments, beads are first surrounded by symmetrical clouds of actin filaments which undergo spontaneous symmetry breaking that can lead to stripping of the actin coat or to directional motion of the beads. The biophysical mechanisms underlying these behaviors depend on the tensile stress that can build up in the actin-network surrounding the bead. Above a critical force value that depends on the actin coat thickness, the network will break at an imperfection. To robustly observe symmetry breaking in these systems, coat polymerization and/or de-polymerization has to be controlled in a way that the coat does not become too thick [103,104], thereby reaching a metastable state where small fluctuations in tensile stress can yield coat rupture.

Results confirming these mechanisms have been reported in a minimal system using an amphiphatic complex of the branched actin polymerizer ActA from *L. monocytogenes* localized to the inner interface of water-in-oil emulsions. Here, actin filaments polymerize and form dynamic cortices by self-organization that only require nucleation factors [105]. In these spherical structures, spontaneous symmetry breaking and formation of polar actin caps can be observed, which depends on temperature and cross-linkers and is generated through myosin dependent cortical flows in absence of any external cues. Moreover, other forms of spontaneous symmetry breaking such as blebbing also occur in this system [105]. Using elasticity theory and linear flux-force relationships, a theoretical model has been built. It posits that interfacial polymerization can trigger an instability which induces spontaneous symmetry breaking [106]. In the light of work from the Schwille group [99] and the model of Lewis *et al.* [107], myosin-mediated actin fragmentation or viscous/elastic stress originating from turnover/de-polymerization might also be possible explanations for spontaneous symmetry breaking observed experimentally in the ActA system.

Thus, under certain conditions, viscous and elastic stresses are sufficient to break symmetry without polarized myosin activity *in vitro*. Although similar stresses are also found *in vivo*, these usually require anisotropic myosin contractility. One explanation for these differences might stem from positive feedback mechanisms and coupling to other cytoskeletal structures, most importantly microtubules, *in vivo*.

A different type of dissipative self-organized structure has been reported from a reconstituted system where meiotic extract is confined to droplets in an emulsion [108]. Here, actomyosin flow generates stable vortices that depend on actin polymerization and de-polymerization. Strikingly, inhibition of either polymerization or de-polymerization leads to collapse of vortices while fusion of two droplets with vortices leads to re-organization of the two halos into one that scales to the size of the droplet [108]. These observations have led to the development of a mathematical model that can explain this emergent phenomenon: Lewis *et al.*, using an isotropic viscoelastic model, show that these dissipative structures can emerge from the viscoelasticity of the system when rearrangements in the actomyosin network are slower than the disassembly rate while not requiring a specific polarity of its constituents [107]. Thus, unlike in the microtubule-motor examples above, polarity sorting does not seem to contribute to formation of mesoscopic structures in this case [60–62].

2.4. Actomyosin in Single Cells

2.4.1. Blebbing and Migration

In cellular systems, spontaneous symmetry breaking can also occur in the form of blebbing [21] (Figure 3a). Here, a biophysical mechanism for bleb formation has been put forward by Charras *et al.* [94]: The important assumption of this model is the cytoplasm resembling a porous elastomer that is contractile and infiltrated with a fluid. If the cortex surrounding such a fluid-filled elastomer locally contracts, the hydrostatic pressure will also locally increase and fluid will flow out of the porous elastomer at a breakpoint in the cortex leading to membrane detachment and blebbing. Importantly, since local cortex contraction and breakpoint can be at some distance and since the tensile force of the cortex is transduced to the elastomer, there is no instantaneous propagation. From this model it is obvious that blebbing can be regulated by altering actomyosin cortex strength (density and thickness), tensile stress (myosin concentration and activation), hydrostatic pressure [101,109–112], and porosity of the elastomer (difficult to modulate *in vivo*).

Symmetry breaking by blebbing can lead to cell migration [113–115] (Figure 3b). This type of cell migration works without classical cell-substrate adhesion—in fact, cells seem to be able to switch between the adhesion-dependent and blebbing-based motility by altering actin polymerization rate [116]. Instead of contraction of the substrate as observed during adhesion-dependent migration, the substrate is expanded during blebbing-based motility [117]. This can lead to surprisingly fast polarized movement if blebbing is maintained by a positive feedback between contractility and cortical flow [18].

Blebbing as a ubiquitous biomechanical mechanism also plays a role in cell-in-cell invasion, also coined entosis [118]. Entosis is an integrin-independent process that seems to be driven by blebbing and a uropod-like actin structure at the rear of the invading cell [96] (Figure 3c). During entosis, fate symmetry breaking is determined by mechanical deformability—highly deformable cells preferentially engulf and out-compete neighboring cells by internalizing and degrading them [119].

In contrast, blebbing can also inhibit spontaneous symmetry breaking by leading to a stabilization of the cleavage furrow, when releasing cortical tension symmetrically [95] (Figure 3d). Hence, inherent instabilities in actomyosin cytoskeletal mechanics can be deployed for symmetry breaking which can have complex consequences during tumorigenesis (entosis), cell division, or migration (blebbing).

Besides blebbing, other forms of actomyosin-based spontaneous symmetry breaking are involved in cell migration (reviewed in [120,121]): While actin polymerization at the future cell front promotes symmetry breaking when chemotactic or other cues are involved, contractility through non-muscle myosin II polarizes the rear of the cell [97,122]. This leads to an anisotropic organization of the cell's actomyosin machinery and drives translocation. Translocation will further reinforce actomyosin asymmetry, favoring further translocation [123] (Figure 3e). Similarly, in three-dimensional environments, both amoeboid and mesenchymal migration start with non-muscle myosin II accumulating at the cell rear to initiate actomyosin contractility which in turn drives cells to move; additionally, mesenchymal migration also requires stress fibers to be generated before directional migration [124]. The force distribution during this type of migration is anisotropic with the front generating traction by actin network-substrate interactions, while the cell's sides and its back produce traction by the actin network slipping over the substrate [125]. Strikingly, it was now shown that spontaneous motility in this case does not originate from rear contraction itself but is initiated by stochastic fluctuations in adhesion strength and myosin localization in the prospective cell rear [98]. This will generate high actin network flow that can trigger a switch in cell adhesion from gripping to slipping. This switch in turn allows flow acceleration resulting in rear retraction. Then, the above mentioned anisotropic state is reached that is self-sustained through additional positive feedback.

The biological relevance of rear contractility-based spontaneous migration is not fully clear yet. It has been proposed to be utilized when cells move away from certain cues, during reverse cell turns, or during cell intercalation [120].

In addition, another component seems to contribute to spontaneous symmetry breaking that triggers cell migration, confinement. Using *D. discoideum* cells, it has been recently demonstrated that cells can spontaneously polarize inside narrow channels in the form of highly persistent, unidirectional migration [126]. Under these conditions, their actin network is organized in dense, stationary actin foci at the sides and an enrichment of non-muscle myosin II at the rear, which is however not required for persistent migration under confinement. The topology of non-muscle myosin II polarization is very similar to stable bleb migration that has been found to stochastically occur in cells of developing embryos under similar confinement [18] and probably in many mesenchymal cells under confinement that use non-muscle myosin II contractility to trigger mechanical instability [127]. However, unlike spontaneous confinement-induced migration in *D. discoideum*, stable bleb migration in vertebrate cells requires long-range cortical flow and depends on non-muscle myosin II activity [18,127].

2.4.2. Defining Singularities in Cells

As briefly explained above, axon specification of neurons in culture also represents a process of spontaneous symmetry breaking where actomyosin plays a key role [66–69] and where a singularity has to emerge from a stochastic process. Current models of this process always require positive feedback but differ in that they either assume competition of each neurite for a limited amount of certain molecules or an activator-inhibitor pair [128]. In the latter model an activator is generated within one neurite and this in turn mounts a global inhibitory signal. In both cases, this will lead to local activation of actin polymerization either in a “one-takes-all” or in a “local activation-global inhibition” mechanism (Figure 4a). Proof for the former mechanisms comes from the finding that H-Ras might indeed be a molecule that is

present in limited amounts [129]. However, it does not seem to influence actin dynamics directly since other Ras isoforms have been shown to act either through GSK3 β signaling [130] or through the actin-binding protein afadin [131].

Following the establishment of a single site for axon formation, actin polymerization and forces generated by non-muscle myosin II in the axonal growth cone lead to retrograde flow, which will lead to protrusion formation when flow is coupled to movement of cell adhesion molecules [132,133] (Figure 4b). This flow induces actin arcs in the transition zone of the growth cone (between the growth cone's center and the ruffled periphery). These arcs inhibit growth of microtubules into the peripheral zone of the growth cone [134]. Further, contractile actin arc structures are regulated by Rho Kinase-mediated non-muscle myosin II activation and indeed coordinate microtubule movements in the growth cone neck [70]: Laterally moving actin arcs interact with growing axonal microtubules and transport them from the sides of the growth cone into the central domain. This led to the conclusion that non-muscle myosin II-dependent compressive forces are necessary for microtubule alignment in the growth cone neck [71].

Taken together, this complex chain of events shows that multiple (potentially redundant) signaling pathways through positive feedback first locally activate retrograde actomyosin flow that then establishes secondary structures like actin arcs. These in turn are important for proper organization of microtubules in the growing axon.

In the asymmetrically dividing budding yeast *S. cerevisiae*, spontaneous symmetry breaking has been extensively studied (Figure 4c). Similar to neurons, a single location has to grow into the bud based on a stochastic process and competition. This process also occurs without an external cue by self-enhancing positive feedback centered on the polarity factor Cdc42, a small, prenylated GTPase that associates with the plasma membrane [11]. Numerous studies have established a mechanism in which recruitment of Cdc42 to the site of polarization (where activated, GTP-bound Cdc42 seems to laterally diffuse, [135]) requires actin-mediated transport of vesicle-bound Cdc42 [136] or GTPase-activating protein (GAP)-mediated recruitment of Cdc42 [137]. In addition, Cdc42 cycling between GTP-bound/active and GDP-bound/inactive states is crucial for polarization, which is controlled by a guanine nucleotide exchange factor (GEF, Cdc24), GAPs (Bem2, Bem3, Rga1, Rga2), a Rho-guanine nucleotide dissociation inhibitor (GDI, Rdi1) [138], and plasma membrane lipid anisotropy [139] (Figure 4d). Recent work has shown that actin-mediated recycling of Cdc42 induces robust symmetry breaking but does not restrict polarization to a single site [6]. A synthetic approach has been used in this case in which the scaffold protein Bem1 (which affects actin filament attachment to the polarization site) was fused to the v-SNARE Snc2 (which very efficiently transports vesicles and slowly diffuses from the site of membrane fusion) (Figure 4e, top). Under these engineered conditions, cells can generate two polarization sites, which when given sufficient time will start to slowly compete and sometimes fail to develop a single polarization site before budding begins [6] (Figure 4e, bottom). Thus, actin-based delivery needs additional inputs to ensure that a singularity emerges from a spontaneous process. This is similar to neurons where a complex machinery—after a spontaneous event—also establishes positive feedback to generate a singularity, which is crucial for proper physiological function of the cell.

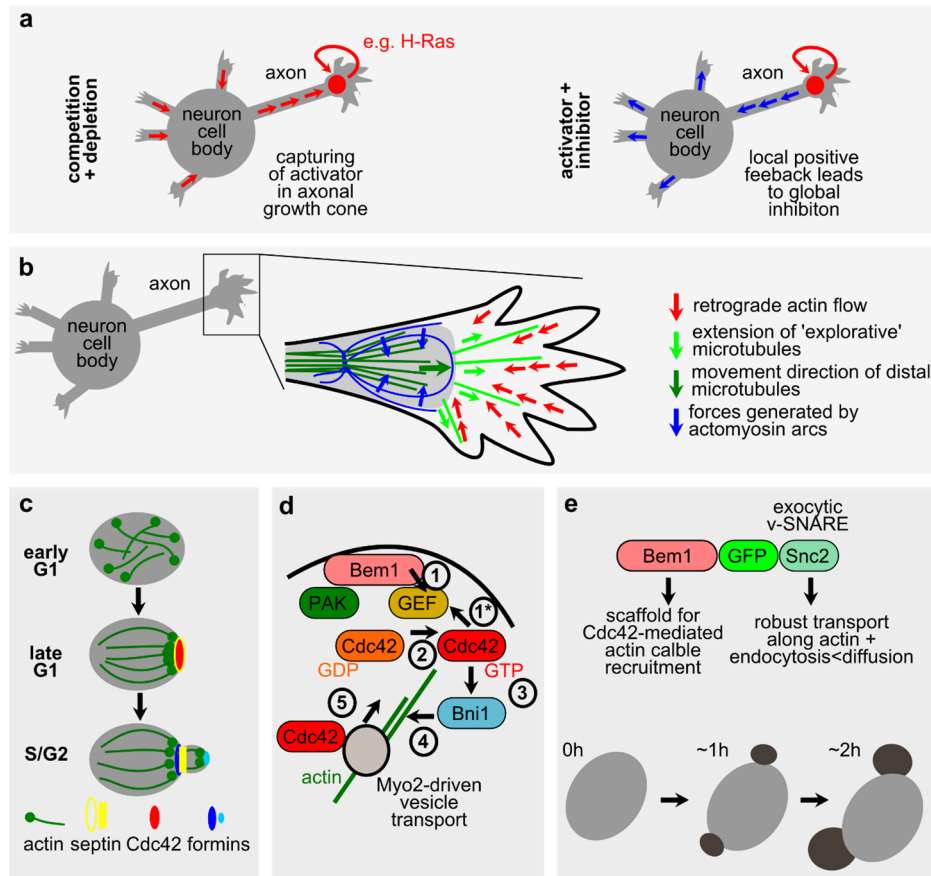


Figure 4. How to generate a singularity in neurons and in *S. cerevisiae*. **(a)** Models that explain the generation of a single axon. Adapted from [128]; see text for details; **(b)** Actomyosin-dependent remodeling of axonal microtubules. The enlarged area shows a schematic that summarizes dynamics during growth cone advancement. Adapted from [70]. In the peripheral domain of the growth cone (right), dynamics microtubules (green arrows) polymerize parallel to filopodial actin filaments that are subject to retrograde flow (red arrows). Therefore, peripheral microtubules cannot reach filopodial tips. Slowing of retrograde flow (not shown) and centripetal forces generated in actomyosin arcs (blue arrows) lead to opening of the central zone (depicted in grey) and microtubule advancement; **(c)** Cell division in *S. cerevisiae*. Note the re-structuring of actin cables and the formation of a bud site that contains Cdc42. At this site, also the septin ring forms (see [12] for details); **(d)** Positive feedback leads to enrichment of Cdc42 at a single site during budding. Schematic adapted from [12]. Cortically bound Cdc42-GTP (bound through stochastic events, **(1*)**) can recruit the cytoplasmically assembled complex of the scaffold protein Bem1 with PAK (Cla4/Ste20) and a Cdc42 guanine nucleotide exchange factor (GEF) (Cdc24) **(1)**. GEF activity leads to local enrichment of Cdc42-GTP **(2)**, thereby establishing positive feedback. Higher amounts of Cdc42-GTP promote recruitment and activation of the formin Bni1 **(3)** that leads to the capture/formation of actin cables **(4)**. Along actin cables, vesicle-bound Cdc42 can be transported (using the myosin motor Myo2, **(5)**). This will lead to further enrichment of Cdc42 and start a second positive feedback; **(e)** Fusion of the scaffold Bem1 to the exocytic v-SNARE Snc2 (top) can lead to the simultaneous formation of two buds (bottom, dark grey). See text and [6] for details.

Remarkably, besides the complex machinery that ensures singularity in the spontaneous polarization process of yeast, polarization can also be triggered by an electric field. Here, bud emergence occurs towards the cell membrane with depolarized potential [140], probably coordinated by plasma membrane lipid polarization [138].

2.5. Actomyosin-Dependent Chiral Symmetry Breaking

A special form of spontaneous symmetry breaking is the generation of chiral symmetry where an initially symmetric state at the mesoscopic level is transformed into a state that shows a particular handedness. This transition is of great importance for cells and organisms since it creates an additional layer of diversification in form and function. The most plausible explanation underlying this phenomenon is that biological systems use homochiral building blocks [141]. From these, macromolecules with specific biases concerning their chirality can be formed. A particular macromolecular handedness can then be propagated either through biochemical reactions or through interaction of handed macromolecules with each other (e.g., through polymerization or formation of active materials at mesoscopic scales).

Filamentous actin fulfills these requirements of an intrinsically chiral macromolecule. It is formed by actin protomers that assemble into a right-handed double helix with a full turn after 13 protomers or every 72 nm [142]. Sequential interactions of myosin motors with one of the helical strands can therefore generate a right-handed rotation of the filament around its axis [143]. Moreover, the myosin working stroke is not perfectly parallel to the axis of the actin filament [144] (and references therein), thus resulting in a small angular component that can generate torque. Torque is clearly seen in *in vitro* assays: Nishizaka *et al.* [145] showed that during myosin-driven sliding of actin filaments, a torque component can be observed that induce rotation of an actin filament around its long axis. Later, Sase *et al.* [143] have confirmed that actin filaments undergo one revolution per sliding distance of approximately 1 μm . Similar rotation or twirling of actin filaments have been confirmed in more recent reports [144,146]. Interestingly, both left-handed and right-handed rotation has been demonstrated (for myosin II and myosin VI, respectively [144,147]). Rotation is insensitive to myosin concentration, filament length, and filament velocity but its handedness depends on the length of the myosin lever arm [144]. In the following two main types of chiral symmetry breaking in single cells will be discussed, spontaneous events and events that are triggered by confinement.

Spontaneous chiral symmetry breaking in actomyosin systems seems to originate from chiral interactions of its constituents. This has been confirmed by the identification of spontaneous chiral transitions in *in vitro* experiments where cells autonomously form asymmetric patterns without directional cues: Neurites of varying origins such as retinal explants [148], retinal ganglion cells [149], neocortical neurons [150], hippocampal explants [151] all show clockwise growth on 2D substrates. This chiral outgrowth of neurites is driven by force generation through filopodia rotation. Since filopodia are actin-rich structures, perturbation of the actin cytoskeleton inhibits neurite turning and the left-handed spiral myosin-V motor generates directionality of rotation [151]. Besides neurons, clockwise rotation of actin bundles also occurs in melanophores [152]. Rotation has also been observed in 3D cultures of glandular cells where single cells undergo multiple rotations and keep rotating cohesively after divisions [153]. However, it seems likely that this intrinsic chirality of cells is not solely rooted in the chirality of actomyosin but also uses the core polarity machinery in conjunction with the microtubule cytoskeleton [154].

Besides spontaneously occurring, chiral behavior of cells can also be induced: Micropatterns mimic tissue architecture by confining cells in certain geometries. Upon meeting boundary restrictions cells are forced to break symmetry to acquire lower energy states. This spontaneous decision seems to be made by almost all cell types and is highly consistent for a given cell type [155–157]. Notably, actin function is critical for chiral transitions on patterned surfaces [155].

More generally, it has been proposed that rotating movements seems to be a general feature of normal epithelial cells when confined [158,159], however, not in transformed cells [153,158]. This behavior can even be further extended to unicellular organisms (e.g., *Dictyostelium discoideum* [160]). As demonstrated theoretically, one possible mechanism underlying rotation seems to be intracellular torque that results from the correlation of actomyosin force vectors in a cell pair (which depends on actomyosin forcing) and interfacial deflection (which depends on cortical tension) [161].

Comprehensive experimental and computational analysis using micro-patterns has provided valuable insights into chiral properties of actin filaments and how they break symmetry [162]. Using adhesive islands, it was shown that actin filaments with focal adhesions transition from an isotropic radial pattern into a chiral pattern with invariant handedness. First, radial actin fibers originate from focal adhesions and polymerize towards the cell center. Formation of self-organized radial actin structures depends on formin, an actin nucleation factor that generates unbranched filaments. Also, active contractile transverse fibers can be observed moving centripetally along radial fibers. Subsequently, radial fibers start to tilt and form a chiral pattern. Centripetal force is generated by actomyosin contractility in transverse fibers moving along radial fibers. Transfer of contractile centripetal stress creates a tangential force leading to chiral tilting or rotational movement of radial fibers. Some of the mechanisms found in this system might also explain the handedness observed for turning of single cells since they might also contain spatially and molecularly polarized actin filaments.

The neutrophil represents a cell type that is well known for chemotaxis-induced polarized migration in the form of biased random walks. Similar to confined epithelial cells, neutrophils in enclosed microfluidic channels show directional symmetry breaking by forming symmetric bifurcations, through splitting of their leading edge [163]. Which branch of the bifurcation is used for further migration is ultimately resolved by a stochastic symmetry-breaking behavior, probably involving actin polymerization similar to axon selection in neurons.

Somewhat similar to neutrophils, human pro-myelocytic leukemia cells (dHL60) respond to a uniform concentration of attractant by migrating leftward to a line connecting the nucleus of the un-polarized cell to its centrosome before start of migration [154]. This bias relies on the GTPase Cdc42, the Par3/Par6/aPKC complex, and the kinase GSK3. In addition, cells lose this directional bias if their microtubules are depolymerized. Xu *et al.* [154] suggested that the centrosome could serve as an intrinsically chiral structure directing polarity in the absence of spatial cues. However, it also seems likely that chirality of the microtubule cytoskeleton itself contributes to leftward bias.

3. Chiral Symmetry Breaking *in Vivo*

3.1. Left/Right (L/R) Asymmetry and the “Conversion Hypothesis”

In most animals, an invariant form of primary L/R asymmetry exists, therefore, most animals are homo-chiral (reviewed in [164]). Invariant asymmetry is rooted in a decision taken during early development. Somewhat surprisingly, this decision is a binary choice since even in homo-chiral animals rare individuals can be found that are mirror-symmetric to the rest of the population, a phenotype called *situs inversus* [165,166]. A *situs inversus* can be functionally equivalent and phenotypically asymptomatic if all L/R asymmetries are inverted, however, if only some L/R asymmetries are inverted, global L/R coordination is usually lost, which leads to severe physiological defects [167,168].

Brown and Wolpert conceived the “conversion hypothesis” to mechanistically explain the origin of organismal chirality and to account for the prevalence of invariant primary L/R asymmetries [169]. They hypothesized that L/R asymmetry develops from an intrinsic property of the developing system and lies at the molecular level. They proposed the existence of a so-called “F-molecule”, a chiral molecule able to orient itself along the anteroposterior (A/P) and dorsoventral (D/V) axes, which were created by external cues and/or inductive signaling. Further, they suggested that the asymmetric structure of the “F-molecule” could cause oriented action along its arms and inadvertently result in polarization along the midline. Like this, an L/R axis is formed. Thus, an “F-molecule” would render a dedicated signaling mechanism for L/R symmetry breaking unnecessary.

Although many biological molecules are asymmetric or chiral, some obvious candidates are cytoskeletal elements as they are capable of producing handed dynamics. Nevertheless, organismal L/R patterning in animals has been previously discussed to be accomplished by mechanisms incompatible with a universal “F-molecule” since it was thought that invertebrates and vertebrates use different mechanisms for L/R patterning. In contrast, solid evidence exists that chirality of the cytoskeleton (representing the “F-molecule”) is mainly responsible for organismal chirality in invertebrates. Moreover, embryonic structure responsible for organismal chirality in vertebrates, the node, a transient embryonic cavity that forms at the anterior end of the developing notochord, seems to use the same cytoskeletal chirality and the same regulatory pathways rendering it L/R asymmetric.

3.2. Chiral Symmetry Breaking in Invertebrates

Famous examples which directly illustrate organismal primary L/R asymmetry emerging during early embryonic development are the leech *Helobdella robusta* [170], the snail *Lymnaea stagnalis* [171], and the nematode *Caenorhabditis elegans* [165]. For *C. elegans* and *L. stagnalis*, it could be demonstrated that early embryonic L/R symmetry breaking requires a particular, transient chiral arrangement of cells in the early embryo affecting all later L/R asymmetries [165,172], including lateralization of the nervous system [173].

3.2.1. Helobdella

The spirally cleaving glossiphoniid leech *Helobdella robusta*, which belongs to the *Lophotrochozoa*, shows asymmetric divisions at the first and second round of cell divisions (unlike the snails discussed below) [174]. During the second round of division, the larger D quadrant is generated on the left side of the embryo, which gives rise to bilaterally symmetric mesoderm/ectoderm tissues and inherits unequally segregated developmental determinants. Unequal cleavage seems to be due to the initially symmetric mitotic apparatus anisotropically extending rightward in an actomyosin-dependent process. Interestingly, a morphological left-right asymmetry is already present in the 2-cell embryo, which precedes cytokinesis and predicts the chirality of the second cleavage [175]. This first asymmetric cleavage is due to transient down-regulation of one centrosome and the partial collapse of its aster [176] and rather insensitive to changes in actomyosin contractility [175]. Hence, symmetry breaking, potentially initiated through asymmetric regulation of microtubule growth/density, is propagated through yet unknown asymmetric regulation of cortical actomyosin to break L/R symmetry. There are, however, also *Lophotrochozoa* where chiral cell arrangements do not seem to be propagated through development [177,178]; it will be interesting to find out how microtubules and actomyosin interact in this system and why chiral cellular configurations do not always establish invariant developmental L/R patterning.

3.2.2. Lymnaea

In the gastropod *Lymnaea stagnalis* and *Lymnaea peregra*, chirality is an inherited trait from a single locus with the sinistral form being recessive and the dextral form being dominant [179–182]. During the third round of embryonic cell divisions in dextral *Lymnaea stagnalis*, spindles twist clockwise and cells deform dextrotropically at the metaphase-anaphase transition (when viewed from the animal pole) In the recessive, sinistral embryos, no counter-clockwise twisting of spindles is found. Instead, chirality only emerges during the furrow ingression when cells deform by turning leftwards [183] (Figure 5a, right). Actin de-polymerization agents alter both cleavages to neutral (Figure 5b, right). Importantly, when pushing the surface of each cell in the directions opposite to the normal third cleavage at the metaphase-anaphase transition (for dextral embryos) or telophase (for sinistral embryos), animals with inverted chirality are obtained [172] (Figure 5c). Although the chirality of cell rotations during the first and second round of cell divisions indicates organismal chirality [184], it does not seem to be directly linked to the decisive event at the third round of division [172]. This has been explained by the chirality at the third round of cell divisions more directly influencing the cell arrangement of the organizer, which emerges at the 24-cell stage [174]. Moreover, asymmetric expression of genes of the Nodal pathway [185], which is a conserved gene expression module operating in *Deuterostomia*, is directly dependent on the chirality of the third round of cell divisions.

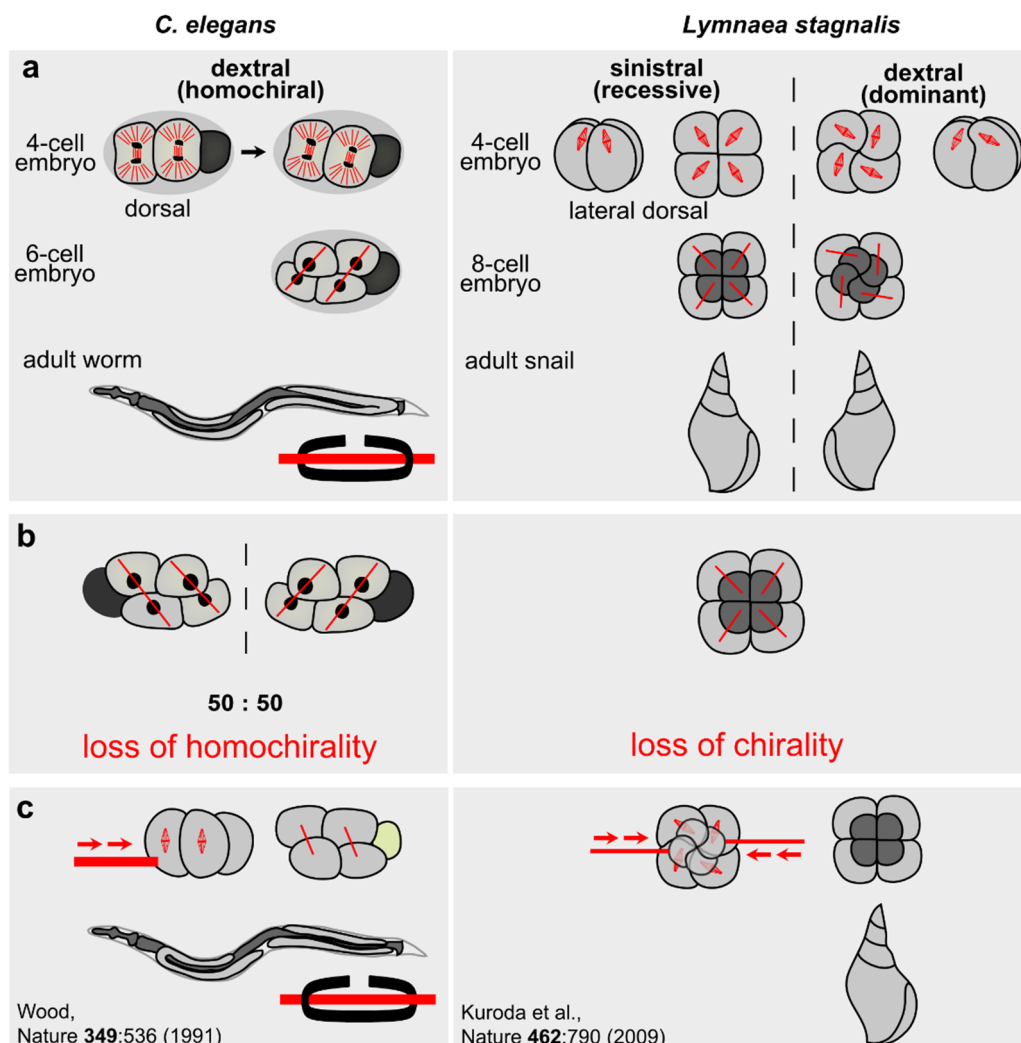


Figure 5. Chiral blastomere arrangements in *C. elegans* and *L. stagnalis* are crucial for L/R patterning (a) Top: Formation of chiral blastomere arrangements during early embryogenesis. The ectodermal founder cells (*C. elegans*) that skew their spindles are shown in light grey, their spindles in red. Middle: Staggered, chiral configurations at the 6-cell stage (*C. elegans*) or third round of division (*L. stagnalis*), daughter cells are connected by a red line. Bottom: Adult worms have an invariant body handedness, manifesting in gonad (black) coiling around the gut (red). See text for details (b) Genetic manipulation or drug treatment can either lead to situs randomization (*C. elegans*) or loss of chirality (*L. stagnalis*) (c) Micromanipulations used to unveil the decisive step in L/R patterning. See text for details.

3.2.3. *C. elegans*

Although active chiral processes play an important role in biological pattern formation [186] (see above), it has been only recently confirmed by Grill and coworkers that the underlying mechanism for cellular chirality in *C. elegans* is rooted in chiral cortical actomyosin dynamics. Grill and coworkers could reveal that chiral dynamics in the actomyosin cortex can be observed already during the initial polarizing flow that generates the A/P axis in the 1-cell embryo [187]. Using active chiral fluid theory,

they proposed that chiral flow is generated by gradients in active torque density along the A/P axis and could demonstrate that Rho signaling controls chiral flows.

In addition to handedness at the 1-cell stage, Wood and coworkers have recently described that at the transition of the 2- to the 3-cell embryo, L/R symmetry is broken concomitantly with establishment of D/V axis polarity during division of the ectodermal founder cell, AB [188]. They suggested that due to L/R asymmetries in the AB cell's cortex, its cleavage furrow initiates asymmetrically, invariably from the left, thereby pre-patterning subsequent events. Moreover, they observed that cortical rotation occurs during the first cleavage with invariant chirality (a clockwise rotation, when viewed from anterior; Figure 6a), which confirms the findings from the Grill lab that the one-cell embryo has an intrinsic chirality [187].

Subsequently, during the division of the two ectodermal founder cells in the *C. elegans* 4-cell embryo, their spindles are first parallel to the L/R axis and then invariantly skew clockwise (with the embryo oriented dorsal up). Like this, the four ectodermal daughters acquire a staggered configuration (Figure 5a, left) [189]. When the actin cytoskeleton is perturbed either by growing embryos at low temperatures (10 °C, [190,191]) or genetically ([191] and unpublished observations), embryos with a mirror-symmetric chiral cell arrangement are obtained. In the case of genetic perturbation, this can lead to a quantitative randomization of adult L/R asymmetries (unpublished observations) (Figure 5b, left). Wood has accomplished a mechanical inversion of the chiral arrangement by micromanipulation of cells and could demonstrate that this leads to L/R inversion in adults. Therefore, the decisive step for L/R symmetry breaking is the chiral cell arrangement in the 6-cell embryo [165] (Figure 5c, left). Furthermore, active torque seems to facilitate L/R symmetry breaking: The clockwise skew of ectodermal cells at the 4- to 6-cell transition (Figure 5a, left) is accompanied by chiral cortical dynamics during cytokinesis in that the cortex in the nascent daughter cells of ABa and ABp show counter-rotating flows [187].

However, although L/R symmetry is broken by chiral flows at the transition from the 4-cell to the 6-cell stage, a chiral morphogenetic process follows that patterns the embryonic L/R axis in *C. elegans* [191]. This process, coined chiral symmetry breaking, directly succeeds spindle skewing of the ectodermal cells at the 6-cell stage and relies on the differential regulation of cortical contractility between the ABpl and ABpr sister cells. Chiral morphogenesis generates rotational force in the embryo that leads to a chiral re-arrangement of cell positions (Figure 6b). Hence, it constitutes a process with torque on a multi-cellular level. This is accomplished by cytoskeletal dynamics generating a chiral cell arrangement and is therefore highly similar to the one breaking symmetry during gastropod development [172,183]. Remarkably, Grill and coworkers could uncover that Wnt signaling known to regulate this chiral symmetry breaking process [191] is also required for chiral flow as early as the 1-cell stage and later for counter-rotating flows during skewing of the ABa/ABp division [187]. Thus, the same genes seem to affect both cortical actomyosin chirality and L/R symmetry breaking. These findings provide further support for the idea that chirality on the molecular level of the cytoskeleton could indeed represent the "F-molecule" responsible for organismal L/R asymmetries.

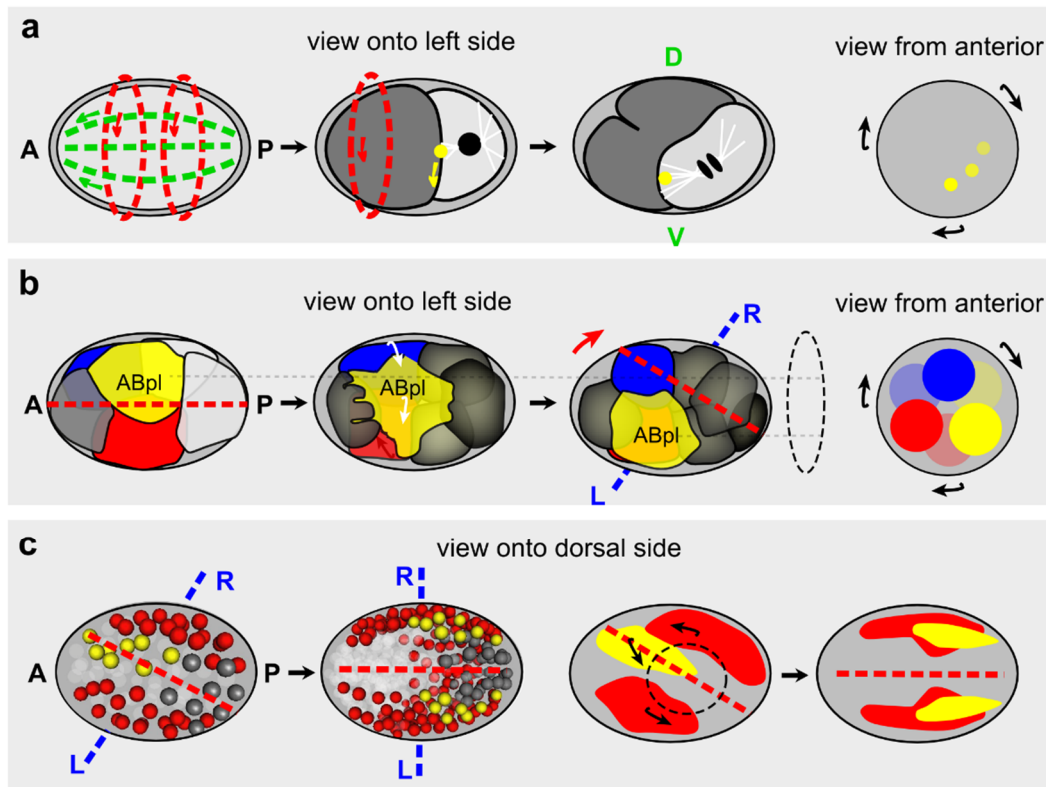


Figure 6. Chiral processes that mediate axis formation and anteroposterior (L/R) asymmetric patterning. (a) Before dorsoventral (D/V) axis formation starts, cortical rotation can be observed in the *C. elegans* embryo (left). This has been interpreted as a first sign of cellular chirality [188]. Cortical rotation occurs again during the next division and re-positions the cell division remnant of the first division (yellow) asymmetrically onto the future ventral side (middle). Due to persistent spindle-cell division remnant interactions, the spindle in the posterior cell (white lines) is also skewed ventrally, thereby generating the invariant configuration of the 4-cell embryo [192,193]; (b) After spindle skewing during the L/R divisions of the two ectodermal founder cells ABa and ABp (see Figure 5a), a chiral morphogenetic process starts (left): The left daughter of ABp, ABpl changes its shape due to differential regulation of cortical actomyosin, and migrates ventrally (middle). Due to asymmetric cell-cell contacts, this leads to a clockwise rotation of cells when viewed from anterior (right); (c) During most of gastrulation, the embryo uses a skewed midline (dashed red line) for asymmetric L/R inductions. Gradually, bilaterally symmetric lineages (red and yellow) undergo a chiral, coordinated transition into a symmetric configuration. See text for details.

Moreover, recent work from Singh and Pohl could uncover how chiral cortical dynamics coordinate D/V and L/R axial patterning (reviewed in [192,194]). During the transition from the 2- to the 3-cell embryo, rotational cortical actomyosin flow, polarized orthogonally to the A/P axis in the ectodermal founder cell AB, positions the cell division remnant of the first cell division onto the future ventral side of the animal [193] (Figure 6a). Perturbation of rotational cortical actomyosin flow revealed that asymmetric cell division remnant positioning is crucial for D/V axis formation. The cell division remnant

serves as a cortical landmark for spindle orientation in the posterior cell, P1, that needs this cue to break the Hertwig rule and rotate its spindle onto the A/P axis (which is the shorter axis of the cell). This ensures successful cell positioning, asymmetric cell division and asymmetric Notch/Wnt inductions [192,193].

Thus, cortical actomyosin regulation through Rho and Wnt signaling ensures proper intracellular chirality. This chirality is then further amplified through cell-cell interactions to chirality on a global scale: Chiral symmetry breaking through cell rotation at the 6-cell stage not only increases L/R asymmetry established by the spindle skewing at the 4- to 6-cell transition but establishes an asymmetrically positioned midline (Figure 6b) [191]. Importantly, this asymmetrically positioned midline is maintained during the time window of all major asymmetric inductions that differentially pattern left and right body halves [195,196]. Due to complex cell rearrangements during late stages of gastrulation, the global asymmetry is gradually transformed into superficial L/R symmetry with a symmetrically positioned midline (Figure 6c, left) [197]. A comprehensive analysis of these cell rearrangements uncovered a chiral collective migration phase which seems to be driven by cortical actomyosin dynamics (Figure 6c, right) [197]. This migration resembles the directional rotation in a plane. Such rotations seem to be generally implicated in active chiral patterning processes *in vivo* [198,199]. As described above, directional rotation in a plane has also been observed in cultured mammalian cells growing on micro-patterns with defined boundaries [155]. Under these conditions, cells form invariant chiral alignments that also rely on actomyosin function.

Collectively, these findings suggest that complex chiral cellular behaviors might deploy intrinsic chirality of actomyosin differentially controlled or coupled spatiotemporally to extrinsic cues, for instance a globally operating signaling system that allows to decode spatial information locally [200–202]. Hence the work in the past years has yielded a quite complete picture of chiral symmetry breaking in *C. elegans*: (1) Cortical chirality seems to constitute the underlying molecular origin for symmetry breaking; (2) cortical chirality can be regulated by changing non-muscle myosin II activation through Rho and Wnt pathways (and probably additional, not yet identified pathways); (3) asymmetric cell-cell interactions amplify intracellular chirality into local and then global chirality. The currently available data allows us to speculate that a similar mechanism also operates in snails.

Nevertheless, it should be noted that (again similar to *Lophotrochozoa*) *Nematoda* exist not developing with invariant handedness and where a chiral cellular arrangement does not seem to be the decisive L/R patterning step also exist [203,204]. It will be interesting to explore (a) whether intracellular chirality on the level of the actomyosin cytoskeleton is modified here; (b) whether intracellular chirality competes with other forms of intracellular chiral systems (e.g., microtubules); or (c) whether different mechanisms of amplification of cellular chirality exist that lead to different mechanisms for global L/R asymmetry.

3.2.4. *D. melanogaster*

Besides *Lophotrochozoa* and *Nematoda*, L/R patterning is also investigated in *Arthropoda*, particularly in *Drosophila melanogaster* [205]. The breakthrough discovery that fueled L/R patterning research was the identification of unconventional myosin ID (myoID/myo31DF) mutants. These show an inversion of the L/R axis and reversal of all L/R asymmetric organs, e.g., gut looping, spermiduct coiling, rotation of the male terminalia [206–208]. MyoID belongs to the class I non-filamentous myosins, which are actin-binding motor proteins known for roles in actin cytoskeleton organization, cell

motility, and endocytosis [209]. Membrane anchored type I myosin can generate chiral actin motility *in vitro* and this chirality is a property of the working stroke of myosin. [210]. Very recently, the Matsuno laboratory has demonstrated that besides MyoID other myosin I motors have overlapping functions with MyoID in tissue chirality [211]. Thus, *D. melanogaster* type I myosins seem to generate chiral forces by interacting with actin filaments.

Unlike in *Lophotrochozoa*, *Nematoda*, or vertebrates (see below), L/R tissue asymmetries do not seem to be coordinated by a decisive step in early embryogenesis or a globally acting L/R organizer. Instead, depletion of MyoID in a tissue-specific manner only leads to the reversal of its lateralization without affecting other tissue L/R asymmetries [206,207].

MyoID function during L/R symmetry breaking also relies on its interaction with β -catenin [212], a key molecule in cell-cell adhesion and Wnt signaling [213]. β -catenin is a component of adherens junctions that also contain E-cadherin and α -catenin. It has been shown that adherens junctions are crucial to transduce L/R asymmetry information [212], and MyoID affects their L/R asymmetric distribution important for maintaining chiral cell shapes [199]. Notably, individual cellular chirality is integrated into planar polarity in the case of hindgut morphogenesis and thereby leads to asymmetric organ patterning [199]. Here, the atypical cadherin Dachous and the Dachous/Fat/Frizzled planar cell polarity pathway (see below) are involved in transducing intracellular information [214]. This pathway is known to be responsible for cytoskeletal organization and junctional remodeling [215]. In later work from the Matsuno laboratory, it was demonstrated that organ handedness is indeed rooted in individual cell chirality, since in genetic mosaics composed of Myo31DF mutant and overexpressing cells only overexpressing cells formed proper cell-shape chirality [216]. In addition, canonical Wnt signaling has also been implicated in L/R organ asymmetry [217]. Thus, although regulated organ-specifically and organ-restricted, intracellular chirality generated by actin-myosin interactions also generates chirality similar to *Lophotrochozoa* and *Nematoda* and uses components of the Wnt pathway important for cellular and organismal chirality in *C. elegans* [164,187,191].

Recently, it has been shown that the well-known transcription factor Abdominal-B operates upstream of MyoID (and possibly also other factors that affect L/R patterning) [218]. This transcription factor is required for myoID expression. Surprisingly, its loss does not lead to reversion of L/R asymmetries like the loss of myoID, rather, L/R asymmetry is lost. Noselli and colleagues have argued that this reveals the existence of a sinistral activity since inversion is only apparent in a myoID mutant context [208].

Furthermore, there are also other recently identified rotational tissue movements in *Drosophila* that mediate morphogenesis: Transition from a round to an elongated egg is driven by polar arrays of microtubules and actomyosin contraction [219–221]. Topologically similar to *C. elegans* cortical rotation [187,188,193], follicles exhibit circumferential rotation around their long (A/P) axis which is used to elongate the egg through deposition of polarized extracellular matrix that constrains tissue shape [219]. Individual egg chambers rotate either in a clockwise or counterclockwise direction and it could be demonstrated that SCAR-dependent lamellipodial leading edges of follicle cells [221] and polarized microtubules are required for rotation [220]. Microtubule polarization precedes the onset of egg chamber rotation and predicts the direction of rotation [220]. Besides generating polarized extracellular matrix, polarized actin bundles form in the follicle epithelium perpendicular to the elongation axis [221]. The rotation itself seems to mediate actin bundling and only becomes dispensable after the basement membrane is polarized [221]. This process also requires the atypical cadherin Fat [220], which is also

involved in L/R symmetry breaking in other organs of *D. melanogaster* (see above, [214]). Interestingly, rotational motion of mammary epithelial acini in 3D environments also leads to extracellular matrix deposition and lack of rotation leads to a loss of matrix deposition [222].

Taken together, *D. melanogaster* also uses the actomyosin cytoskeleton to generate chirality, however, in a cell-type specific manner and modulated by additional accessory factors.

3.2.5. Helical Growth Mutants from the Plant *A. thaliana* and Their Effects on Invertebrate Chirality

Most of the above findings feature actomyosin as the cytoskeletal system involved in cellular, organ, or organismal chirality. Microtubules are much less studied in this context but also seem to play a conserved role in contributing to L/R asymmetries: The Levin laboratory could demonstrate that mutations in α -tubulin (TUA4 and TUA6) [223] and mutations in a γ -tubulin-associated protein (tortifolia1/Tubgcp2) [224] that had been previously shown to generate helical growth in the plant *Arabidopsis thaliana* alter organismal L/R patterning in *C. elegans* and vertebrates (see below) [225]. They generated a D256A/E259A double mutation in the *tba-9* gene (orthologous to *A. thaliana* TUA6), coding for one of nine α -tubulins in *C. elegans*. When expressed in a neuron pair that stochastically establishes L/R asymmetric cell identities, similar levels of randomization as previously accomplished by microtubule de-polymerization [226] were reached. Furthermore, they used the neutrophil cell line HL60 as *in vitro* system (introduced above in Section 2.2; [154]) and found that the leftward bias is lost when mutated Tub- α 6 is expressed [225]. Notably, the TUA4 (tortifolia2) mutant phenotype is most likely due to a loss of α -tubulin forming hydrogen bonds with the GTPase domain of β -tubulin which seems to lead to a handed twisting of isolated cells [227]. Consistent with patterning of dense microtubule arrays by gravity (see above, [47–49]), hypergravity induces reorientation of cortical microtubules in plant cells from transverse to longitudinal which is greatly exaggerated in α -tubulin mutants [228]. Thus, in addition to actomyosin, microtubule structure can directly contribute to cellular chirality. Although these findings are in line with aspects of microtubule behavior observed *in vitro* [47–49], the underlying mechanisms how microtubules generate chirality in animals and how chirality is amplified to the tissue and organ level are not yet clear, especially since plant cell cortical microtubules are contributing to cell shape symmetry breaking through mechanisms not present in animals [229].

3.3. Chiral Symmetry Breaking in Vertebrates

In vertebrates, almost all organs are L/R asymmetric. Evidence that cytoskeletal proteins play a role in establishing these asymmetries emerged with the report of dysfunctional cilia causing *situs inversus totalis* [230]. In the 1990s it became clear that directional flow in the ciliated node (functionally orthologous structures are also called Hensen's node, Kupffer's vesicle, or dorsal blastopore lip), a transient embryonic structure that forms at the anterior end of the primitive streak in a gastrulating embryo mediates L/R symmetry breaking through establishment of L/R asymmetric gene expression (reviewed in [231–234]). The rotating monocilia of the late gastrula node are microtubule-based structures that differ from regular motile cilia in that they are only composed of nine peripheral microtubule doublets but lack the central pair of singlets. L/R asymmetric gene expression requires clockwise beating of cilia in the node, thereby generating leftward flow [235–240]; if rightward flow is generated mechanically, this leads to *situs inversus* [241]. Directional flow activates the conserved Nodal signaling pathway

which leads to L/R asymmetric expression of genes during early embryogenesis even before any morphological L/R asymmetries manifest [242–245]. Two biochemical/biophysical mechanisms have evolved that explain how directional nodal flow might lead to L/R asymmetric gene expression through the Nodal pathway; these mechanisms are however not compatible [233]. (1) In the experimentally less well supported morphogen mechanism, leftward nodal flow will lead to directional transport of morphogen(s) to the left side of the node, probably in the form of “nodal vesicular parcels” [246], however, a 100-fold reduction of nodal cilia is still sufficient to drive L/R symmetry breaking [247]. In this scenario, insufficient flow will be generated to drive directional transport of large cargo; (2) The experimentally more thoroughly supported two-cilia mechanism requires that flow generated by clockwise beating central nodal monocilia (with small magnitudes likely being sufficient) is sensed by peripheral immotile sensory cilia in order for L/R patterning to occur correctly [233,248].

Notwithstanding the controversy which of the two models is correct, there is also ample evidence that cell- or tissue-intrinsic mechanisms using the actin cytoskeleton contribute to L/R patterning either through affecting patterning of the node [198] or by promoting organ chirality independently of Nodal signaling [249]. Specifically, Gros *et al.* have argued that mesodermal nodal cells in the chick embryo do not have cilia and that the short cilia on endodermal nodal cells are unrelated to mesodermal motile cilia in mammals. This interpretation has been recently confirmed [250]. Interestingly, Gros *et al.* could demonstrate that the node’s L/R asymmetry is crucial for L/R asymmetric gene expression. This asymmetry is mediated by a non-muscle myosin II-dependent morphogenetic mechanism of asymmetric collective cell migration [198]. Remarkably, in the pig embryo, nodal flow is most likely also absent but the node itself is again L/R asymmetric, suggesting that even in other mammals nodal cilia-dependent flow does not cause chiral symmetry breaking [198]. Additionally, also in ciliated nodes like the zebrafish Kupffer’s vesicle, a non-muscle myosin II-dependent morphogenetic mechanism mediates cellular asymmetry that generates morphological asymmetry [251]. This has led to the conclusion that regional cell shape changes generate L/R organizer asymmetry which is in turn required for asymmetric fluid flow [251]. Moreover, dextral looping of the zebrafish heart seems to arise from a tissue intrinsic process that depends on actomyosin activity, which is enhanced by Nodal signaling [249]. The disruption of actin or myosin II activity, even in presence of asymmetric Nodal signaling, causes defects in organ laterality [249,252]. These findings suggest that the origin of organ laterality can be rooted in actomyosin activity. Thus, it seems that nodal flow might be a secondary mechanism to enforce or further amplify L/R asymmetric information but that actomyosin-mediated asymmetric morphogenesis of the L/R organizer or chiral organs is directly involved in organismal chiral symmetry breaking

It should also be noted that other, earlier forms of chiral cytoskeletal symmetry breaking have been reported in vertebrates, however, different than for invertebrates, these earlier asymmetric processes do most likely not constitute decisive events for organismal L/R patterning [253]. Notably, Danilchik *et al.* have shown that cleaving *Xenopus* embryos undergo a dramatic large-scale torsion, with the actomyosin cortex shearing in an exclusively counterclockwise direction [254]. These dynamics are similar to what has now been demonstrated for torque generation during cell divisions in the early *C. elegans* embryo [187] and suggest that vertebrate embryonic cells might also possess intrinsic chirality. Moreover, as introduced above, injection of mRNA coding for orthologs of the *A. thaliana* helical growth mutant α -tubulin or mutant γ -tubulin associated protein Tubgcp2 in one-cell *X. laevis* embryos leads to heterotaxia, possibly through altered microtubule-based transport and actin organization in the early embryo [225].

In sum, a model that unites vertebrate and invertebrate chiral symmetry breaking seems to emerge: While intracellular chirality (rooted predominantly in the actomyosin cytoskeleton) is amplified through cell-cell contacts in Invertebrates and leads to chiral cellular organization [187,191,193,199], cellular chirality in vertebrates can lead to similar chiral tissue dynamics [198]. However, it is currently not clear whether chiral tissue dynamics are a common feature in vertebrates and at what stage of development or organogenesis they matter. Nonetheless, chiral cellular dynamics seem to need further amplification through additional mechanisms like nodal flow (Figure 7). These additional mechanisms might be necessitated by tissue/organ size or compositional complexity. It will therefore be crucial to analyze organ asymmetries quantitatively and with cellular resolution, which has also been key to uncover organismal asymmetries and L/R patterning mechanisms in invertebrates [165,174].

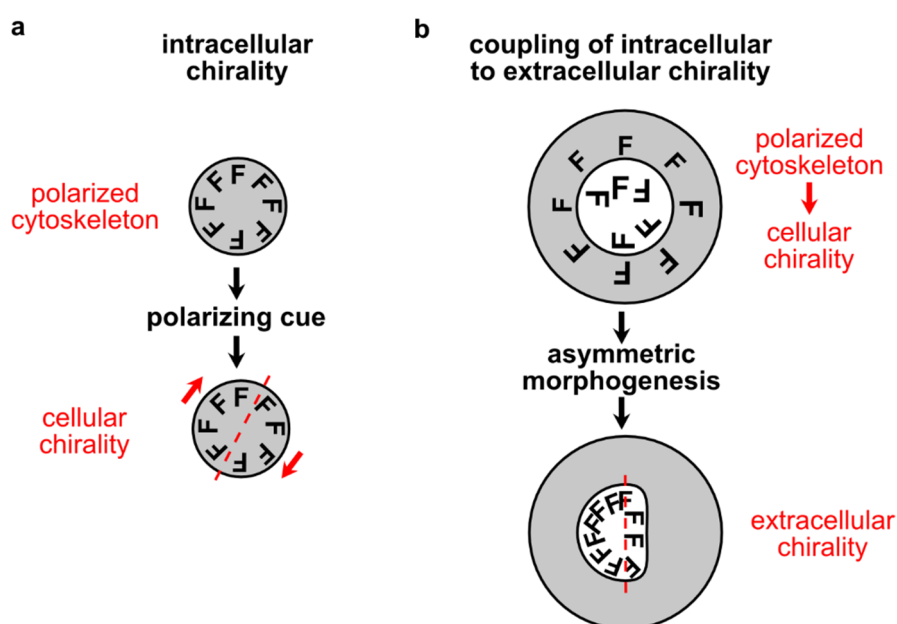


Figure 7. Models for chiral symmetry breaking in invertebrates and vertebrates **(a)** during invertebrate symmetry breaking, an external cue seems to be used in conjunction with an intracellular, chiral structure to generate cellular chirality. Cellular chirality is then used to generate chiral tissue/organ patterns (*D. melanogaster*) or global chirality in the embryo (*C. elegans*, *L. stagnalis*); **(b)** Similarly, cellular chirality is also used in vertebrate symmetry breaking to generate an asymmetric node. Directional flow in the node can then further amplify symmetry breaking.

4. Inductive Polarity and Symmetry Breaking

4.1. Actomyosin

Cortical actomyosin can undergo local contractions that generate surface waves and streaming of the cytoplasm, a phenomenon that has been coined cortical flow [255]. Although the actomyosin cortex has been described as a contractile superficial gel over 70 years ago [256], we have only very recently begun to understand how global aspects of cell behavior are triggered by cortical flow, namely by a gradient in actomyosin contractility to drive flow and a sufficiently large viscosity of the cortex to allow flow to be long-ranged [13]. Patterning of all three major body axes, which are established in first three

consecutive divisions of embryogenesis, relies on cortical actomyosin activity in *C. elegans* [5,7,8,25,26]. The inductive cue that established polarity in this system is sperm entry which triggers anteriorly directed flows in actomyosin cortex in the 1-cell *C. elegans* embryo through the RhoGAP CYK-4 [14,15,255,257–261]. These anteriorly directed flows are advective causing segregation of anterior and posterior polarity domains [16]. Grill and coworkers could demonstrate that cortical flows are fast enough and polarity proteins' cortical association long enough that advection directly affects their distribution. Moreover, the system (1) is multistable and shows hysteresis to avoid polarization in response to fluctuations; and (2) its steady state is determined by front-stalling behavior due to depletion of cytoplasmic protein pools. With these characteristics, contractile cortical flow can serve as a mechanical patterning system that polarizes the embryo independently of polarity proteins directly binding to cortical actomyosin [16].

Following A/P polarization, chiral cortical actomyosin activity patterns the D/V and L/R axes [187,188,191,192,197] (see above), and cortical contractility drives cell internalization and most likely also cell sorting during gastrulation [197,262–267]. The central inductive cue(s) that drives non-muscle myosin II activation during gastrulation is constituted by Wnt signaling [200,265]. This function of Wnt seems to be conserved during later development [268] and among animals: Wnt signaling can cell-autonomously modulate actomyosin distribution, activity, and apical-basal polarization [269,270], and Wnt/planar cell polarity pathway components also seem to directly modulate actin dynamics [271]. Notably, an ancestral Wnt-like system in *D. discoideum* is responsible for actomyosin-mediated morphogenesis [272]. Hence, although the precise cues that establish Wnt signaling in animal development are not clear in all cases, it can be assumed that Wnt/planar cell polarity signaling is a universal cue to deploy actomyosin activity for polarization.

Similar to *C. elegans*, *D. melanogaster* also uses actin for embryonic polarization, however, the cue in this case is not sperm entry but inductive signaling and asymmetric transport of maternal mRNAs during oogenesis—there is no evidence for anterior-directed contractile cortical flow; reviewed in [273,274]. The cortical actin network is however directly responsible for localization of the polarity factor Par1 [275] and together with polarized localization of the polarity regulator Cdc42 involved in oocyte polarization through positive feedback onto the Par3/Par6/aPKC polarity complex [276].

Originating in the Kiehart [277,278] and Wieschaus laboratories [279–281], the role of actomyosin activity during gastrulation movements has been studied in great detail [282–290]: (1) Similar to *C. elegans* [257,258], cortical actomyosin contractility generates system-level hydrodynamic flow [289]; (2) anisotropic pulsatile actomyosin contractility (cell deformations followed by stabilization phases) results in irreversible cell shape changes [285,289]; (3) self-organized anisotropic force distribution regulates cell shape and cell-cell interactions [280,283,284,286,290].

The Zallen laboratory has recently uncovered that spatiotemporal regulation of signaling through the Toll family of receptors is responsible for actomyosin-driven junctional remodeling and axis elongation, thereby identifying a mechanism how axial information can be translated into morphogenetic force [17].

In other organisms, for instance epiboly during zebrafish gastrulation or mouse oocyte polarization, actin dynamics also contribute to polarization and the underlying biomechanical mechanisms are uncovered [291,292]. However, the spatiotemporal cues that initiate these polarized tissue movements are not well understood [292,293] and other pathways than those discussed above might also directly contribute to actomyosin-driven polarization in animals [294].

Taken together, data from spontaneously polarizing systems and developing systems that use a polarization cue are highly consistent in that (1) tuning the threshold(s) in this metastable system through differential control of actin polymerization/cross-linking or non-muscle myosin II activation and (2) self-organization at the level of actomyosin mechanobiology and molecular interactions (both in *cis* and *trans*) are sufficient to drive symmetry breaking. Stochastically emerging anisotropies that occur in *in vitro* systems are transformed into directional processes *in vivo* through spatially patterning the system. Spatial patterning can bias stochastic events mainly by locally altering threshold/activation properties.

4.2. Microtubules: Spindles and Centrosomes

As briefly mentioned above, microtubules can transduce asymmetric information into asymmetric morphogenesis, thus rarely cause symmetry breaking *in vivo* themselves. Nonetheless, microtubules also have essential functions during inductive polarization. In addition to cortical actomyosin flows, microtubules can also organize A/P polarity in *C. elegans* [26,80]. Motegi *et al.* could demonstrate that the centrosome of the sperm can generate two polarity domains in the embryo by centrosomally nucleated microtubules locally protecting PAR-2 from phosphorylation by aPKC [80]. Other microtubule functions in *C. elegans* cell and tissue polarization are coupled to Wnt activity and affect asymmetric cell division [295–300]. These functions seem to be conserved in mammals [301]. Work from the Sawa lab could now uncover that asymmetric cortical localization of the Wnt pathway component Adenomatous polyposis coli (APC) can directly regulate spindle asymmetry [302]. Strikingly, Sawa and coworkers could also reverse mutant phenotypes by manipulating spindle asymmetry with laser ablations of centrosomes, confirming that asymmetric microtubule distribution is crucial for asymmetric cell division [302].

Other processes where microtubules decode inductive signals are symmetric and asymmetric stem cell divisions [303–306] and symmetric cell divisions under the control of the Wnt/planar cell polarity pathway [307–309]. Interestingly, the latter type of regulation is responsible for asymmetric positioning of motile cilia [19,20,310]. Thus, “decoding” of polarity cues by microtubules is a wide-spread phenomenon in animals. However, evidence is still sparse that microtubules themselves can initiate polarity in a self-organized fashion *in vivo*.

In future, it will be necessary to more closely inspect the mechanobiology of actomyosin-microtubule interactions *in vivo* and to combine microtubule- and actomyosin-based systems *in vitro*. Such approaches might lead to the identification of previously overlooked emergent phenomena or mechanisms of self-organization, and might identify additional symmetry breaking mechanisms.

Acknowledgments

C.P. wants to thank the reviewers and all members of his laboratory for ideas and comments. Research in the laboratory of C.P. is funded by the Deutsche Forschungsgemeinschaft (EXC 115, FOR 1756) and the LOEWE Research Cluster Ubiquitin Networks. C.P. is supported by a European Union Framework Program 7 fellowship (Marie Curie Actions Project 326632).

Conflicts of Interest

The author declares no conflict of interest.

References

1. Li, R.; Bowerman, B. Symmetry breaking in biology. *Cold Spring Harb. Perspect. Biol.* **2010**, *2*, doi:10.1101/cshperspect.a003475.
2. Wodarz, A. Establishing cell polarity in development. *Nat. Cell Biol.* **2002**, *4*, E39–E44.
3. Meinhardt, H. Models for the generation and interpretation of gradients. *Cold Spring Harb. Perspect. Biol.* **2009**, *1*, doi:10.1101/cshperspect.a001362.
4. Meinhardt, H. Models of biological pattern formation: From elementary steps to the organization of embryonic axes. *Curr. Top. Dev. Biol.* **2008**, *81*, 1–63.
5. Nance, J.; Zallen, J.A. Elaborating polarity: PAR proteins and the cytoskeleton. *Development* **2011**, *138*, 799–809.
6. Howell, A.S.; Savage, N.S.; Johnson, S.A.; Bose, I.; Wagner, A.W.; Zyla, T.R.; Nijhout, H.F.; Reed, M.C.; Goryachev, A.B.; Lew, D.J. Singularity in polarization: Rewiring yeast cells to make two buds. *Cell* **2009**, *139*, 731–743.
7. Li, R.; Gundersen, G.G. Beyond polymer polarity: How the cytoskeleton builds a polarized cell. *Nat. Rev. Mol. Cell Biol.* **2008**, *9*, 860–873.
8. Cowan, C.R.; Hyman, A.A. Acto-myosin reorganization and PAR polarity in *C. elegans*. *Development* **2007**, *134*, 1035–1043.
9. Van Amerongen, R.; Nusse, R. Towards an integrated view of Wnt signaling in development. *Development* **2009**, *136*, 3205–3214.
10. Greenwald, I. Notch and the awesome power of genetics. *Genetics* **2012**, *191*, 655–669.
11. Wedlich-Söldner, R.; Altschuler, S.; Wu, L.; Li, R. Spontaneous cell polarization through actomyosin-based delivery of the Cdc42 GTPase. *Science* **2003**, *299*, 1231–1235.
12. Bi, E.; Park, H.O. Cell polarization and cytokinesis in budding yeast. *Genetics* **2012**, *191*, 347–387.
13. Mayer, M.; Depken, M.; Bois, J.S.; Jülicher, F.; Grill, S.W. Anisotropies in cortical tension reveal the physical basis of polarizing cortical flows. *Nature* **2010**, *467*, 617–621.
14. Munro, E.; Nance, J.; Priess, J.R. Cortical flows powered by asymmetrical contraction transport PAR proteins to establish and maintain anterior-posterior polarity in the early *C. elegans* embryo. *Dev. Cell* **2004**, *7*, 413–424.
15. Jenkins, N.; Saam, J.R.; Mango, S.E. CYK-4/GAP provides a localized cue to initiate anteroposterior polarity upon fertilization. *Science* **2006**, *313*, 1298–1301.
16. Goehring, N.W.; Trong, P.K.; Bois, J.S.; Chowdhury, D.; Nicola, E.M.; Hyman, A.A.; Grill, S.W. Polarization of PAR proteins by advective triggering of a pattern-forming system. *Science* **2011**, *334*, 1137–1141.
17. Paré, A.C.; Vichas, A.; Fincher, C.T.; Mirman, Z.; Farrell, D.L.; Mainieri, A.; Zallen, J.A. A positional Toll receptor code directs convergent extension in *Drosophila*. *Nature* **2014**, *515*, 523–527.
18. Ruprecht, V.; Wieser, S.; Callan-Jones, A.; Smutny, M.; Morita, H.; Sako, K.; Barone, V.; Ritsch-Marte, M.; Sixt, M.; Voituriez, R.; *et al.* Cortical contractility triggers a stochastic switch to fast amoeboid cell motility. *Cell* **2015**, *160*, 673–685.

19. Hashimoto, M.; Shinohara, K.; Wang, J.; Ikeuchi, S.; Yoshida, S.; Meno, C.; Nonaka, S.; Takada, S.; Hatta, K.; Wynshaw-Boris, A.; *et al.* Planar polarization of node cells determines the rotational axis of node cilia. *Nat. Cell Biol.* **2010**, *12*, 170–176.
20. Borovina, A.; Superina, S.; Voskas, D.; Ciruna, B. Vangl2 directs the posterior tilting and asymmetric localization of motile primary cilia. *Nat. Cell Biol.* **2010**, *12*, 407–412.
21. Van der Gucht, J.; Sykes, C. Physical model of cellular symmetry breaking. *Cold Spring Harb. Perspect. Biol.* **2009**, *1*, doi:10.1101/cshperspect.a001909.
22. Lancaster, M.A.; Knoblich, J.A. Organogenesis in a dish: Modeling development and disease using organoid technologies. *Science* **2014**, *345*, doi:10.1126/science.1247125.
23. Turing, A.M. The chemical basis of morphogenesis. *Philosoph. Trans. R. Soc. Lond.* **1952**, *237*, 37–72.
24. Ladewig, J.; Koch, P.; Brüstle, O. Leveling Waddington: The emergence of direct programming and the loss of cell fate hierarchies. *Nat. Rev. Mol. Cell Biol.* **2013**, *14*, 225–236.
25. Fievet, B.T.; Rodriguez, J.; Naganathan, S.; Lee, C.; Zeiser, E.; Ishidate, T.; Shirayama, M.; Grill, S.; Ahringer, J. Systematic genetic interaction screens uncover cell polarity regulators and functional redundancy. *Nat. Cell Biol.* **2013**, *15*, 103–112.
26. Motegi, F.; Seydoux, G. The PAR network: Redundancy and robustness in a symmetry-breaking system. *Philos. Trans. R. Soc. Lond. B Biol. Sci.* **2013**, *368*, doi:10.1098/rstb.2013.0010.
27. Mitchison, T.; Kirschner, M. Dynamic instability of microtubule growth. *Nature* **1984**, *312*, 237–242.
28. Mitchison, T.; Kirschner, M. Microtubule assembly nucleated by isolated centrosomes. *Nature* **1984**, *312*, 232–237.
29. Kirschner, M.; Mitchison, T. Beyond self-assembly: From microtubules to morphogenesis. *Cell* **1986**, *45*, 329–342.
30. Padinhateeri, R.; Kolomeisky, A.B.; Lacoste, D. Random hydrolysis controls the dynamic instability of microtubules. *Biophys. J.* **2012**, *102*, 1274–1283.
31. Bayley, P.M.; Schilstra, M.J.; Martin, S.R. A simple formulation of microtubule dynamics: Quantitative implications of the dynamic instability of microtubule populations *in vivo* and *in vitro*. *J. Cell Sci.* **1989**, *93*, 241–254.
32. Dogterom, M.; Leibler, S. Physical aspects of the growth and regulation of microtubule structures. *Phys. Rev. Lett.* **1993**, *70*, 1347–1350.
33. Flyvbjerg, H.; Holy, T.E.; Leibler, S. Stochastic dynamics of microtubules: A model for caps and catastrophes. *Phys. Rev. Lett.* **1994**, *73*, 2372–2375.
34. Margolin, G.; Gregoret, I.V.; Goodson, H.V.; Alber, M.S. Analysis of a mesoscopic stochastic model of microtubule dynamic instability. *Phys. Rev. E Stat. Nonlinear Soft Matter Phys.* **2006**, *74*, doi:10.1103/PhysRevE.74.041920.
35. Zong, C.; Lu, T.; Shen, T.; Wolynes, P.G. Nonequilibrium self-assembly of linear fibers: Microscopic treatment of growth, decay, catastrophe and rescue. *Phys. Biol.* **2006**, *3*, 83–92.
36. Antal, T.; Krapivsky, P.L.; Redner, S.; Mailman, M.; Chakraborty, B. Dynamics of an idealized model of microtubule growth and catastrophe. *Phys. Rev. E Stat. Nonlinear Soft Matter Phys.* **2007**, *76*, doi:10.1103/PhysRevE.76.041907.
37. Ranjith, P.; Lacoste, D.; Mallick, K.; Joanny, J.F. Nonequilibrium self-assembly of a filament coupled to ATP/GTP hydrolysis. *Biophys. J.* **2009**, *96*, 2146–2159.

38. Kueh, H.Y.; Mitchison, T.J. Structural plasticity in actin and tubulin polymer dynamics. *Science* **2009**, *325*, 960–963.
39. Wang, H.W.; Nogales, E. Nucleotide-dependent bending flexibility of tubulin regulates microtubule assembly. *Nature* **2005**, *435*, 911–915.
40. Brouhard, G.J.; Rice, L.M. The contribution of $\alpha\beta$ -tubulin curvature to microtubule dynamics. *J. Cell Biol.* **2014**, *207*, 323–334.
41. Zhang, R.; Alushin, G.M.; Brown, A.; Nogales, E. Mechanistic origin of microtubule dynamic instability and its modulation by EB proteins. *Cell* **2015**, *162*, 849–859.
42. Carlier, M.F.; Melki, R.; Pantaloni, D.; Hill, T.L.; Chen, Y. Synchronous oscillations in microtubule polymerization. *Proc. Natl. Acad. Sci. USA* **1987**, *84*, 5257–5261.
43. Pirollet, F.; Job, D.; Margolis, R.L.; Garel, J.R. An oscillatory mode for microtubule assembly. *EMBO J.* **1987**, *6*, 3247–3252.
44. Tabony, J.; Job, D. Spatial structures in microtubular solutions requiring a sustained energy source. *Nature* **1990**, *346*, 448–451.
45. Mandelkow, E.; Mandelkow, E.M.; Hotani, H.; Hess, B.; Müller, S.C. Spatial patterns from oscillating microtubules. *Science* **1989**, *246*, 1291–1293.
46. Buxbaum, R.E.; Dennerll, T.; Weiss, S.; Heidemann, S.R. F-actin and microtubule suspensions as indeterminate fluids. *Science* **1987**, *235*, 1511–1514.
47. Tabony, J.; Job, D. Gravitational symmetry breaking in microtubular dissipative structures. *Proc. Natl. Acad. Sci. USA* **1992**, *89*, 6948–6952.
48. Papaseit, C.; Pochon, N.; Tabony, J. Microtubule self-organization is gravity-dependent. *Proc. Natl. Acad. Sci. USA* **2000**, *97*, 8364–8368.
49. Tuszynski, J.A.; Sataric, M.V.; Portet, S.; Dixon, J.M. Gravitational symmetry breaking leads to a polar liquid crystal phase of microtubules *in vitro*. *J. Biol. Phys.* **2005**, *31*, 477–486.
50. Yokota, H.; Neff, A.W.; Malacinski, G.M. Early development of *Xenopus* embryos is affected by simulated gravity. *Adv. Space Res.* **1994**, *14*, 249–255.
51. Nouri, C.; Tuszynski, J.A.; Wiebe, M.W.; Gordon, R. Simulation of the effects of microtubules in the cortical rotation of amphibian embryos in normal and zero gravity. *Biosystems* **2012**, *109*, 444–449.
52. Tabony, J.; Rigotti, N.; Glade, N.; Cortès, S. Effect of weightlessness on colloidal particle transport and segregation in self-organising microtubule preparations. *Biophys. Chem.* **2007**, *127*, 172–180.
53. Reber, S.B.; Baumgart, J.; Widlund, P.O.; Pozniakovsky, A.; Howard, J.; Hyman, A.A.; Jülicher, F. XMAP215 activity sets spindle length by controlling the total mass of spindle microtubules. *Nat. Cell Biol.* **2013**, *15*, 1116–1122.
54. Brugués, J.; Needleman, D. Physical basis of spindle self-organization. *Proc. Natl. Acad. Sci. USA* **2014**, *111*, 18496–18500.
55. Schliwa, M.; Woehlke, G. Molecular motors. Switching on kinesin. *Nature* **2001**, *411*, 424–425.
56. Nédélec, F.J.; Surrey, T.; Maggs, A.C.; Leibler, S. Self-organization of microtubules and motors. *Nature* **1997**, *389*, 305–308.
57. Surrey, T.; Nédélec, F.; Leibler, S.; Karsenti, E. Physical properties determining self-organization of motors and microtubules. *Science* **2001**, *292*, 1167–1171.

58. Nogales, E. An electron microscopy journey in the study of microtubule structure and dynamics. *Protein Sci.* **2015**, doi:10.1002/pro.2808.
59. Millecamps, S.; Julien, J.P. Axonal transport deficits and neurodegenerative disease. *Nat. Rev. Neurosci.* **2013**, *14*, 161–176.
60. Sanchez, T.; Chen, D.T.; DeCamp, S.J.; Heymann, M.; Dogic, Z. Spontaneous motion in hierarchically assembled active matter. *Nature* **2012**, *491*, 431–434.
61. Keber, F.C.; Loiseau, E.; Sanchez, T.; de Camp, S.J.; Giomi, L.; Bowick, M.J.; Marchetti, M.C.; Dogic, Z.; Bausch, A.R. Topology and dynamics of active nematic vesicles. *Science* **2014**, *345*, 1135–1139.
62. Sumino, Y.; Nagai, K.H.; Shitaka, Y.; Tanaka, D.; Yoshikawa, K.; Chaté, H.; Oiwa, K. Large-scale vortex lattice emerging from collectively moving microtubules. *Nature* **2012**, *483*, 448–452.
63. Serbus, L.R.; Cha, B.J.; Theurkauf, W.E.; Saxton, W.M. Dynein and the actin cytoskeleton control kinesin-driven cytoplasmic streaming in *Drosophila* oocytes. *Development* **2005**, *132*, 3743–3752.
64. Wasteneys, G.O.; Ambrose, J.C. Spatial organization of plant cortical microtubules: Close encounters of the 2D kind. *Trends Cell Biol.* **2009**, *19*, 62–71.
65. Sanchez, T.; Welch, D.; Nicastro, D.; Dogic, Z. Cilia-like beating of active microtubule bundles. *Science* **2011**, *333*, 456–459.
66. Dotti, C.G.; Banker, G.A. Experimentally induced alteration in the polarity of developing neurons. *Nature* **1987**, *330*, 254–256.
67. Forscher, P.; Smith, S.J. Actions of cytochalasins on the organization of actin filaments and microtubules in a neuronal growth cone. *J. Cell Biol.* **1988**, *107*, 1505–1516.
68. Andersen, S.S.; Bi, G.Q. Axon formation: A molecular model for the generation of neuronal polarity. *Bioessays* **2000**, *22*, 172–179.
69. Bradke, F.; Dotti, C.G. The role of local actin instability in axon formation. *Science* **1999**, *283*, 1931–1934.
70. Schaefer, A.W.; Schoonderwoert, V.T.; Ji, L.; Medeiros, N.; Danuser, G.; Forscher, P. Coordination of actin filament and microtubule dynamics during neurite outgrowth. *Dev. Cell* **2008**, *15*, 146–162.
71. Burnette, D.T.; Ji, L.; Schaefer, A.W.; Medeiros, N.A.; Danuser, G.; Forscher, P. Myosin II activity facilitates microtubule bundling in the neuronal growth cone neck. *Dev. Cell* **2008**, *15*, 163–169.
72. Witte, H.; Neukirchen, D.; Bradke, F. Microtubule stabilization specifies initial neuronal polarization. *J. Cell Biol.* **2008**, *180*, 619–632.
73. Seetapun, D.; Odde, D.J. Cell-length-dependent microtubule accumulation during polarization. *Curr. Biol.* **2010**, *20*, 979–988.
74. Goldstein, B.; Macara, I.G. The PAR proteins: Fundamental players in animal cell polarization. *Dev. Cell* **2007**, *13*, 609–622.
75. Kemphues, K. PARsing embryonic polarity. *Cell* **2000**, *101*, 345–348.
76. Shi, S.H.; Jan, L.Y.; Jan, Y.N. Hippocampal neuronal polarity specified by spatially localized mPar3/mPar6 and PI 3-kinase activity. *Cell* **2003**, *112*, 63–75.
77. Chen, S.; Chen, J.; Shi, H.; Wei, M.; Castaneda-Castellanos, D.R.; Bultje, R.S.; Pei, X.; Kriegstein, A.R.; Zhang, M.; Shi, S.H. Regulation of microtubule stability and organization by mammalian Par3 in specifying neuronal polarity. *Dev. Cell* **2013**, *24*, 26–40.

78. Hu, C.K.; Coughlin, M.; Field, C.M.; Mitchison, T.J. Cell polarization during monopolar cytokinesis. *J. Cell Biol.* **2008**, *181*, 195–202.
79. Rankin, K.E.; Wordeman, L. Long astral microtubules uncouple mitotic spindles from the cytokinetic furrow. *J. Cell Biol.* **2010**, *190*, 35–43.
80. Motegi, F.; Zonies, S.; Hao, Y.; Cuenca, A.A.; Griffin, E.; Seydoux, G. Microtubules induce self-organization of polarized PAR domains in *Caenorhabditis elegans* zygotes. *Nat. Cell Biol.* **2011**, *13*, 1361–1367.
81. Insolera, R.; Chen, S.; Shi, S.H. Par proteins and neuronal polarity. *Dev. Neurobiol.* **2011**, *71*, 483–494.
82. Salbreux, G.; Charras, G.; Paluch, E. Actin cortex mechanics and cellular morphogenesis. *Trends Cell Biol.* **2012**, *22*, 536–545.
83. Heisenberg, C.P.; Bellaïche, Y. Forces in tissue morphogenesis and patterning. *Cell* **2013**, *23*, 948–962.
84. Murrell, M.; Oakes, P.W.; Lenz, M.; Gardel, M.L. Forcing cells into shape: The mechanics of actomyosin contractility. *Nat. Rev. Mol. Cell Biol.* **2015**, *16*, 486–498.
85. Goehring, N.W.; Grill, S.W. Cell polarity: Mechanochemical patterning. *Trends Cell Biol.* **2013**, *23*, 72–80.
86. Grill, S.W. Growing up is stressful: Biophysical laws of morphogenesis. *Curr. Opin. Genet. Dev.* **2011**, *21*, 647–652.
87. Gardel, M.L.; Shin, J.H.; MacKintosh, F.C.; Mahadevan, L.; Matsudaira, P.; Weitz, D.A. Elastic behavior of cross-linked and bundled actin networks. *Science* **2004**, *304*, 1301–1305.
88. Salbreux, G.; Prost, J.; Joanny, J.F. Hydrodynamics of cellular cortical flows and the formation of contractile rings. *Phys. Rev. Lett.* **2009**, *103*, doi:10.1103/PhysRevLett.103.058102.
89. Dalhaimer, P.; Discher, D.E.; Lubensky, T.C. Crosslinked actin networks show liquid crystal elastomer behaviour, including soft-mode elasticity. *Nat. Phys.* **2007**, *3*, 354–360.
90. Wagner, B.; Tharmann, R.; Haase, I.; Fischer, M.; Bausch, A.R. Cytoskeletal polymer networks: The molecule structure of cross-linkers determines macroscopic properties. *Proc. Natl. Acad. Sci. USA* **2006**, *103*, 13974–13978.
91. Vogel, S.K.; Schwille, P. Minimal systems to study membrane-cytoskeleton interactions. *Curr. Opin. Biotechnol.* **2012**, *23*, 758–765.
92. Vogel, S.K.; Heinemann, F.; Chwastek, G.; Schwille, P. The design of MACs (minimal actin cortices). *Cytoskeleton* **2013**, *70*, 706–717.
93. Schaller, V.; Weber, C.; Semmrich, C.; Frey, E.; Bausch, A.R. Polar patterns of driven filaments. *Nature* **2010**, *467*, 73–77.
94. Charras, G.T.; Yarrow, J.C.; Horton, M.A.; Mahadevan, L.; Mitchison, T.J. Non-equilibration of hydrostatic pressure in blebbing cells. *Nature* **2005**, *435*, 365–369.
95. Sedzinski, J.; Biro, M.; Oswald, A.; Tinevez, J.Y.; Salbreux, G.; Paluch, E. Polar actomyosin contractility destabilizes the position of the cytokinetic furrow. *Nature* **2011**, *476*, 462–466.
96. Purvanov, V.; Holst, M.; Khan, J.; Baarlink, C.; Grosse, R. G-protein-coupled receptor signaling and polarized actin dynamics drive cell-in-cell invasion. *Elife* **2014**, *3*, doi: 10.7554/eLife.02786.

97. Yam, P.T.; Wilson, C.A.; Ji, L.; Hebert, B.; Barnhart, E.L.; Dye, N.A.; Wiseman, P.W.; Danuser, G.; Theriot, J.A. Actin-myosin network reorganization breaks symmetry at the cell rear to spontaneously initiate polarized cell motility. *J. Cell Biol.* **2007**, *178*, 1207–1221.
98. Barnhart, E.; Lee, K.C.; Allen, G.M.; Theriot, J.A.; Mogilner, A. Balance between cell-substrate adhesion and myosin contraction determines the frequency of motility initiation in fish keratocytes. *Proc. Natl. Acad. Sci. USA* **2015**, *112*, 5045–5050.
99. Vogel, S.K.; Petrasek, Z.; Heinemann, F.; Schwille, P. Myosin motors fragment and compact membrane-bound actin filaments. *Elife* **2013**, *2*, doi:10.7554/eLife.00116.
100. Carvalho, K.; Tsai, F.C.; Lees, E.; Voituriez, R.; Koenderink, G.H.; Sykes, C. Cell-sized liposomes reveal how actomyosin cortical tension drives shape change. *Proc. Natl. Acad. Sci. USA* **2013**, *110*, 16456–16461.
101. Carvalho, K.; Lemièrre, J.; Faqir, F.; Manzi, J.; Blanchoin, L.; Plastino, J.; Betz, T.; Sykes, C. Actin polymerization or myosin contraction: Two ways to build up cortical tension for symmetry breaking. *Philos. Trans. R. Soc. Lond. B Biol. Sci.* **2013**, *368*, doi:10.1098/rstb.2013.0005.
102. Van Oudenaarden, A.; Theriot, J.A. Cooperative symmetry-breaking by actin polymerization in a model for cell motility. *Nat. Cell Biol.* **1999**, *1*, 493–499.
103. Van der Gucht, J.; Paluch, E.; Plastino, J.; Sykes, C. Stress release drives symmetry breaking for actin-based movement. *Proc. Natl. Acad. Sci. USA* **2005**, *102*, 7847–7852.
104. Sekimoto, K.; Prost, J.; Jülicher, F.; Boukellal, H.; Bernheim-Grosswasser, A. Role of tensile stress in actin gels and a symmetry-breaking instability. *Eur. Phys. J. E Soft Matter* **2004**, *13*, 247–259.
105. Abu Shah, E.; Keren, K. Symmetry breaking in reconstituted actin cortices. *Elife* **2014**, *3*, doi:10.7554/eLife.01433.
106. John, K.; Peyla, P.; Kassner, K.; Prost, J.; Misbah, C. Nonlinear study of symmetry breaking in actin gels: Implications for cellular motility. *Phys. Rev. Lett.* **2008**, *100*, doi:10.1103/PhysRevLett.100.068101.
107. Lewis, O.L.; Guy, R.D.; Allard, J.F. Actin-myosin spatial patterns from a simplified isotropic viscoelastic model. *Biophys. J.* **2014**, *107*, 863–870.
108. Pinot, M.; Steiner, V.; Dehapiot, B.; Yoo, B.K.; Chesnel, F.; Blanchoin, L.; Kervrann, C.; Gueroui, Z. Confinement induces actin flow in a meiotic cytoplasm. *Proc. Natl. Acad. Sci. USA* **2012**, *109*, 11705–11710.
109. Cunningham, C.C. Actin polymerization and intracellular solvent flow in cell surface blebbing. *J. Cell Biol.* **1995**, *129*, 1589–1599.
110. Mills, J.C.; Stone, N.; Erhardt, J.; Pittman, R.N. Apoptotic membrane blebbing is regulated by myosin light chain phosphorylation. *J. Cell Biol.* **1998**, *140*, 627–636.
111. Miyoshi, H.; Umeshita, K.; Sakon, M.; Imajoh-Ohmi, S.; Fujitani, K.; Gotoh, M.; Oiki, E.; Kambayashi, J.; Monden, M. Calpain activation in plasma membrane bleb formation during tert-butyl hydroperoxide-induced rat hepatocyte injury. *Gastroenterology* **1996**, *110*, 1897–1904.
112. Sahai, E.; Marshall, C.J. Differing modes of tumour cell invasion have distinct requirements for Rho/ROCK signaling and extracellular proteolysis. *Nat. Cell Biol.* **2003**, *5*, 711–719.
113. Paluch, E.; Sykes, C.; Prost, J.; Bornens, M. Dynamic modes of the cortical actomyosin gel during cell locomotion and division. *Trends Cell Biol.* **2006**, *16*, 5–10.

114. Yoshida, K.; Soldati, T. Dissection of amoeboid movement into two mechanically distinct modes. *J. Cell Sci.* **2006**, *119*, 3833–3844.
115. Lämmermann, T.; Sixt, M. Mechanical modes of “amoeboid” cell migration. *Curr. Opin. Cell Biol.* **2009**, *21*, 636–644.
116. Renkawitz, J.; Schumann, K.; Weber, M.; Lämmermann, T.; Pflücke, H.; Piel, M.; Polleux, J.; Spatz, J.P.; Sixt, M. Adaptive force transmission in amoeboid cell migration. *Nat. Cell Biol.* **2009**, *11*, 1438–1443.
117. Bergert, M.; Erzberger, A.; Desai, R.A.; Aspalter, I.M.; Oates, A.C.; Charras, G.; Salbreux, G.; Paluch, E.K. Force transmission during adhesion-independent migration. *Nat. Cell Biol.* **2015**, *17*, 524–529.
118. Florey, O.; Krajcovic, M.; Sun, Q.; Overholtzer, M. Entosis. *Curr. Biol.* **2010**, *20*, R88–R89.
119. Sun, Q.; Luo, T.; Ren, Y.; Florey, O.; Shirasawa, S.; Sasazuki, T.; Robinson, D.N.; Overholtzer, M. Competition between human cells by entosis. *Cell Res.* **2014**, *24*, 1299–1310.
120. Cramer, L.P. Forming the cell rear first: Breaking cell symmetry to trigger directed cell migration. *Nat. Cell Biol.* **2010**, *12*, 628–632.
121. Cramer, L.P. Mechanism of cell rear retraction in migrating cells. *Curr. Opin. Cell Biol.* **2013**, *25*, 591–599.
122. Mseka, T.; Bamberg, J.R.; Cramer, L.P. ADF/cofilin family proteins control formation of oriented actin filament bundles in the cell body to trigger fibroblast polarization. *J. Cell Sci.* **2007**, *120*, 4332–4344.
123. Verkhovskiy, A.B.; Svitkina, T.M.; Borisy, G.G. Selfpolarization and directional motility of cytoplasm. *Curr. Biol.* **1999**, *9*, 11–20.
124. Chi, Q.; Yin, T.; Gregersen, H.; Deng, X.; Fan, Y.; Zhao, J.; Liao, D.; Wang, G. Rear actomyosin contractility-driven directional cell migration in three-dimensional matrices: A mechano-chemical coupling mechanism. *J. R. Soc. Interface* **2014**, *11*, doi:10.1098/rsif.2013.1072.
125. Fournier, M.F.; Sauser, R.; Ambrosi, D.; Meister, J.-J.; Verkhovskiy, A.B. Force transmission in migrating cells. *J. Cell Biol.* **2010**, *188*, 287–297.
126. Nagel, O.; Guven, C.; Theves, M.; Driscoll, M.; Losert, W.; Beta, C. Geometry-driven polarity in motile amoeboid cells. *PLoS ONE* **2014**, *9*, doi:10.1371/journal.pone.0113382.
127. Liu, Y.J.; le Berre, M.; Lautenschlaeger, F.; Maiuri, P.; Callan-Jones, A.; Heuzé, M.; Takaki, T.; Voituriez, R.; Piel, M. Confinement and low adhesion induce fast amoeboid migration of slow mesenchymal cells. *Cell* **2015**, *160*, 659–672.
128. Inagaki, N.; Toriyama, M.; Sakumura, Y. Systems biology of symmetry breaking during neuronal polarity formation. *Dev. Neurobiol.* **2011**, *71*, 584–593.
129. Fivaz, M.; Bandara, S.; Inoue, T.; Meyer, T. Robust neuronal symmetry breaking by Ras-triggered local positive feedback. *Curr. Biol.* **2008**, *18*, 44–50.
130. Oinuma, I.; Katoh, H.; Negishi, M. R-Ras controls axon specification upstream of glycogen synthase kinase-3 β through integrin-linked kinase. *J. Biol. Chem.* **2007**, *282*, 303–318.
131. Iwasawa, N.; Negishi, M.; Oinuma, I. R-Ras controls axon branching through afadin in cortical neurons. *Mol. Biol. Cell* **2012**, *23*, 2793–2804.
132. Mitchison, T.; Kirschner, M. Cytoskeletal dynamics and nerve growth. *Neuron* **1988**, *1*, 761–772.

133. Shimada, T.; Toriyama, M.; Uemura, K.; Kamiguchi, H.; Sugiura, T.; Watanabe, N.; Inagaki, N. Shootin1 interacts with actin retrograde flow and L1-CAM to promote axon outgrowth. *J. Cell Biol.* **2008**, *181*, 817–829.
134. Neukirchen, D.; Bradke, F. Neuronal polarization and the cytoskeleton. *Semin. Cell Dev. Biol.* **2011**, *22*, 825–833.
135. Bendezú, F.O.; Vincenzetti, V.; Vavylonis, D.; Wyss, R.; Vogel, H.; Martin, S.G. Spontaneous Cdc42 polarization independent of GDI-mediated extraction and actin-based trafficking. *PLoS Biol.* **2015**, *13*, doi:10.1371/journal.pbio.1002097.
136. Wedlich-Söldner, R.; Wai, S.C.; Schmidt, T.; Li, R. Robust cell polarity is a dynamic state established by coupling transport and GTPase signaling. *J. Cell Biol.* **2004**, *166*, 889–900.
137. Irazoqui, J.E.; Gladfelter, A.S.; Lew, D.J. Scaffold-mediated symmetry breaking by Cdc42p. *Nat. Cell Biol.* **2003**, *5*, 1062–1070.
138. Freisinger, T.; Klünder, B.; Johnson, J.; Müller, N.; Pichler, G.; Beck, G.; Costanzo, M.; Boone, C.; Cerione, R.A.; Frey, E.; Wedlich-Söldner, R. Establishment of a robust single axis of cell polarity by coupling multiple positive feedback loops. *Nat. Commun.* **2013**, *4*, doi:10.1038/ncomms2795.
139. Fairn, G.D.; Hermansson, M.; Somerharju, P.; Grinstein, S. Phosphatidylserine is polarized and required for proper Cdc42 localization and for development of cell polarity. *Nat. Cell Biol.* **2011**, *13*, 1424–1430.
140. Haupt, A.; Campetelli, A.; Bonazzi, D.; Piel, M.; Chang, F.; Minc, N. Electrochemical regulation of budding yeast polarity. *PLoS Biol.* **2014**, *12*, doi:10.1371/journal.pbio.1002029.
141. Blackmond, G. The origin of biological homochirality. *Cold Spring Harb. Perspect. Biol.* **2010**, *2*, 2787–2884.
142. Holmes, K.C.; Popp, D.; Gebhard, W.; Kabsch, W. Atomic model of the actin filament. *Nature* **1990**, *347*, 44–49.
143. Sase, I.; Miyata, H.; Ishiwata, S.; Kinosita, K., Jr. Axial rotation of sliding actin filaments revealed by single-fluorophore imaging. *Proc. Natl. Acad. Sci. USA* **1997**, *94*, 5646–5650.
144. Beausang, J.F.; Schroeder, H.W., III; Nelson, P.C.; Goldman, Y.E. Twirling of actin by myosins II and V observed via polarized TIRF in a modified gliding assay. *Biophys. J.* **2008**, *95*, 5820–5831.
145. Nishizaka, T.; Yagi, T.; Tanaka, Y.; Ishiwata, S. Right-handed rotation of an actin filament in an *in vitro* motile system. *Nature* **1993**, *361*, 269–271.
146. Vilfan, A. Twirling motion of actin filaments in gliding assays with nonprocessive Myosin motors. *Biophys. J.* **2009**, *97*, 1130–1137.
147. Sun, Y.; Schroeder, H.W., III; Beausang, J.F.; Homma, K.; Ikebe, M.; Goldman, Y.E. Myosin VI walks “wiggly” on actin with large and variable tilting. *Mol. Cell* **2007**, *28*, 954–964.
148. Heacock, A.M.; Agranoff, B.W. Clockwise growth of neurites from retinal explants. *Science* **1977**, *198*, 64–66.
149. Schwartz, M.; Agranoff, B.W. Outgrowth and maintenance of neurites from cultured goldfish retinal ganglion cells. *Brain Res.* **1981**, *206*, 331–343.
150. Romijn, H.J.; Mud, M.T.; Wolters, P.S.; Corner, M.A. Neurite formation in dissociated cerebral cortex *in vitro*: Evidence for clockwise outgrowth and autotopic contacts. *Brain Res.* **1980**, *192*, 575–580.

151. Tamada, A.; Kawase, S.; Murakami, F.; Kamiguchi, H. Autonomous right-screw rotation of growth cone filopodia drives neurite turning. *J. Cell Biol.* **2010**, *188*, 429–441.
152. Yamanaka, H.; Kondo, S. Rotating pigment cells exhibit an intrinsic chirality. *Genes Cells* **2015**, *20*, 29–35.
153. Tanner, K.; Mori, H.; Mroue, R.; Bruni-Cardoso, A.; Bissell, M.J. Coherent angular motion in the establishment of multicellular architecture of glandular tissues. *Proc. Natl. Acad. Sci. USA* **2012**, *109*, 1973–1978.
154. Xu, J.; van Keymeulen, A.; Wakida, N.M.; Carlton, P.; Berns, M.W.; Bourne, H.R. Polarity reveals intrinsic cell chirality. *Proc. Natl. Acad. Sci. USA* **2007**, *104*, 9296–9300.
155. Wan, L.Q.; Ronaldson, K.; Park, M.; Taylor, G.; Zhang, Y.; Gimble, J.M.; Vunjak-Novakovic, G. Micropatterned mammalian cells exhibit phenotype-specific left-right asymmetry. *Proc. Natl. Acad. Sci. USA* **2011**, *108*, 12295–12300.
156. Wan, L.Q.; Ronaldson, K.; Guirguis, M.; Vunjak-Novakovic, G. Micropatterning of cells reveals chiral morphogenesis. *Stem Cell Res. Ther.* **2013**, *4*, 24.
157. Chen, T.H.; Hsu, J.J.; Zhao, X.; Guo, C.; Wong, M.N.; Huang, Y.; Li, Z.; Garfinkel, A.; Ho, C.M.; Tintut, Y.; *et al.* Left-right symmetry breaking in tissue morphogenesis via cytoskeletal mechanics. *Circ. Res.* **2012**, *110*, 551–559.
158. Rørth, P. Fellow travellers: Emergent properties of collective cell migration. *EMBO Rep.* **2012**, *13*, 984–991.
159. Doxzen, K.; Vedula, S.R.K.; Leong, M.C.; Hirata, H.; Gov, N.; Kabla, A.J.; Ladoux, B.; Lim, C.T. Guidance of collective cell migration by substrate geometry. *Integr. Biol.* **2013**, *5*, 1026–1035.
160. Rappel, W.-J.; Nicol, A.; Sarkissian, A.; Levine, H.; Loomis, W.F. Self-organized vortex state in two-dimensional *Dictyostelium* dynamics. *Phys. Rev. Lett.* **1999**, *83*, 1247–1250.
161. Leong, F.Y. Physical explanation of coupled cell-cell rotational behavior and interfacial morphology: A particle dynamics model. *Biophys. J.* **2013**, *105*, 2301–2311.
162. Tee, Y.H.; Shemesh, T.; Thiagarajan, V.; Hariadi, R.F.; Anderson, K.L.; Page, C.; Volkmann, N.; Hanein, D.; Sivaramakrishnan, S.; Kozlov, M.M.; *et al.* Cellular chirality arising from the self-organization of the actin cytoskeleton. *Nat. Cell Biol.* **2015**, *17*, 445–457.
163. Ambravaneswaran, V.; Wong, I.Y.; Aranyosi, A.J.; Toner, M.; Irimia, D. Directional decisions during neutrophil chemotaxis inside bifurcating channels. *Integr. Biol.* **2010**, *2*, 639–647.
164. Pohl, C. Left-right patterning in the *C. elegans* embryo: Unique mechanisms and common principles. *Commun. Integr. Biol.* **2011**, *4*, 1–7.
165. Wood, W.B. Evidence from reversal of handedness in *C. elegans* embryos for early cell interactions determining cell fates. *Nature* **1991**, *349*, 536–538.
166. McManus, C. Reversed bodies, reversed brains and (some) reversed behaviors: Of zebrafish and men. *Dev. Cell* **2005**, *8*, 796–797.
167. Sutherland, M.J.; Ware, S.M. Disorders of left-right asymmetry: Heterotaxy and situs inversus. *Am. J. Med. Genet. C Semin. Med. Genet.* **2009**, *151*, 307–317.
168. Yost, H.J. Coordinating the development of bilateral symmetry and left-right asymmetry. *Semin. Cell Dev. Biol.* **2009**, *20*, 455.
169. Brown, N.; Wolpert, L. The development of handedness in left/right asymmetry. *Development* **1990**, *109*, 1–9.

170. Weisblat, D.A. Asymmetric cell divisions in the early embryo of the leech *Helobdella robusta*. *Prog. Mol. Subcell Biol.* **2007**, *45*, 79–95.
171. Crampton, H. Reversal of cleavage in a sinistral gastropod. *Ann. N. Y. Acad. Sci.* **1894**, *8*, 167–170.
172. Kuroda, R.; Endo, B.; Abe, M.; Shimizu, M. Chiral blastomere arrangement dictates zygotic left-right asymmetry pathway in snails. *Nature* **2009**, *462*, 790–794.
173. Poole, R.J.; Hobert, O. Early embryonic programming of neuronal left/right asymmetry in *C. elegans*. *Curr. Biol.* **2006**, *16*, 2279–2292.
174. Freeman, G.; Lundelius, J.W. Evolutionary implications of the mode of D quadrant specification in coelomates with spiral cleavage. *J. Evol. Biol.* **1992**, *5*, 205–247.
175. Lyons, D.C.; Weisblat, D.A. D quadrant specification in the leech *Helobdella*: Actomyosin contractility controls the unequal cleavage of the CD blastomere. *Dev. Biol.* **2009**, *334*, 46–58.
176. Ren, X.; Weisblat, D.A. Asymmetrization of first cleavage by transient disassembly of one spindle pole aster in the leech *Helobdella robusta*. *Dev. Biol.* **2006**, *292*, 103–115.
177. Luetjens, C.M. Multiple, alternative cleavage patterns precede uniform larval morphology during normal development of *Dreissena polymorpha* (Mollusca, Lamellibranchia). *Wilhelm Roux Arch. Dev. Biol.* **1995**, *205*, 138–149.
178. Luetjens, C.M.; Dorresteijn, A.W.C. The site of fertilisation determines dorsoventral polarity but not chirality in the zebra mussel embryo. *Zygote* **1998**, *6*, 125–135.
179. Boycott, A.E.; Diver, C.; Garstang, S.L.; Hardy, A.C.; Turner, F.M. The inheritance of sinistrality in *Lymnaea peregra*. *Phil. Trans. R. Soc. Lond. B* **1930**, *219*, 51–131.
180. Sturtevant, A.H. Inheritance of direction of coiling in *Lymnaea*. *Science* **1923**, *58*, 269–270.
181. Freeman, G.; Lundelius, J.W. The developmental genetics of dextrality and sinistrality in the gastropod *Lymnaea peregra*. *Wilhelm Roux Arch. Dev. Biol.* **1982**, *191*, 69–83.
182. Hosoiri, Y.; Harada, Y.; Kuroda, R. Construction of a backcross progeny collection of dextral and sinistral individuals of a freshwater gastropod, *Lymnaea stagnalis*. *Dev. Genes Evol.* **2003**, *213*, 193–198.
183. Shibazaki, Y.; Shimizu, M.; Kuroda, R. Body handedness is directed by genetically determined cytoskeletal dynamics in the early embryo. *Curr. Biol.* **2004**, *14*, 1462–1467.
184. Meshcheryakov, V.N.; Belousov, L.V. Asymmetrical rotations of blastomeres in early cleavage of gastropoda. *Wilhelm Roux Arch. Dev. Biol.* **1975**, *177*, 193–203.
185. Grande, C.; Patel, N.H. Nodal signalling is involved in left-right asymmetry in snails. *Nature* **2009**, *457*, 1007–1011.
186. Fürthauer, S.; Stempel, M.; Grill, S.W.; Jülicher, F. Active chiral fluids. *Eur. Phys. J. E Soft Matter* **2012**, *35*, 89.
187. Naganathan, S.R.; Fürthauer, S.; Nishikawa, M.; Jülicher, F.; Grill, S.W. Active torque generation by the actomyosin cell cortex drives left-right symmetry breaking. *Elife* **2014**, *3*, doi:10.7554/eLife.04165.
188. Schonegg, S.; Hyman, A.A.; Wood, W.B. Timing and mechanism of the initial cue establishing handed left-right asymmetry in *Caenorhabditis elegans* embryos. *Genesis* **2014**, *52*, 572–580.
189. Bergmann, D.C.; Lee, M.; Robertson, B.; Tsou, M.F.; Rose, L.S.; Wood, W.B. Embryonic handedness choice in *C. elegans* involves the Galpha protein GPA-16. *Development* **2003**, *130*, 5731–5740.

190. Wood, W.B.; Bergmann, D.; Florance, A. Maternal effect of low temperature on handedness determination in *C. elegans* embryos. *Dev. Genet.* **1996**, *19*, 222–230.
191. Pohl, C.; Bao, Z. Chiral forces organize left-right patterning in *C. elegans* by uncoupling midline and anteroposterior axis. *Dev. Cell* **2010**, *19*, 402–412.
192. Singh, D.; Pohl, C. A function for the midbody remnant in embryonic patterning. *Commun. Integr. Biol.* **2014**, *7*, doi:10.4161/cib.28533.
193. Singh, D.; Pohl, C. Coupling of rotational cortical flow, asymmetric midbody positioning, and spindle rotation mediates dorsoventral axis formation in *C. elegans*. *Dev. Cell* **2014**, *28*, 253–267.
194. Pinheiro, D.; Bellaïche, Y. Making the most of the midbody remnant: Specification of the dorsal-ventral axis. *Dev. Cell* **2014**, *28*, 219–220.
195. Hutter, H.; Schnabel, R. *glp-1* and inductions establishing embryonic axes in *C. elegans*. *Development* **1994**, *120*, 2051–2064.
196. Hutter, H.; Schnabel, R. Establishment of left-right asymmetry in the *Caenorhabditis elegans* embryo: A multistep process involving a series of inductive events. *Development* **1995**, *121*, 3417–3424.
197. Pohl, C.; Tjongson, M.; Moore, J.L.; Santella, A.; Bao, Z. Actomyosin-based self-organization of cell internalization during *C. elegans* gastrulation. *BMC Biol.* **2012**, *10*, doi:10.1186/1741-7007-10-94.
198. Gros, J.; Feistel, K.; Viebahn, C.; Blum, M.; Tabin, C.J. Cell movements at Hensen’s node establish left/right asymmetric gene expression in the chick. *Science* **2009**, *324*, 941–944.
199. Taniguchi, K.; Maeda, R.; Ando, T.; Okumura, T.; Nakazawa, N.; Hatori, R.; Nakamura, M.; Hozumi, S.; Fujiwara, H.; Matsuno, K. Chirality in planar cell shape contributes to left-right asymmetric epithelial morphogenesis. *Science* **2011**, *333*, 339–341.
200. Bischoff, M.; Schnabel, R. A posterior centre establishes and maintains polarity of the *Caenorhabditis elegans* embryo by a Wnt-dependent relay mechanism. *PLoS Biol.* **2006**, *4*, doi:10.1371/journal.pbio.0040396.
201. Bischoff, M.; Schnabel, R. Global cell sorting is mediated by local cell-cell interactions in the *C. elegans* embryo. *Dev. Biol.* **2006**, *294*, 432–444.
202. Schnabel, R.; Bischoff, M.; Hintze, A.; Schulz, A.K.; Hejnowicz, A.; Meinhardt, H.; Hutter, H. Global cell sorting in the *C. elegans* embryo defines a new mechanism for pattern formation. *Dev. Biol.* **2006**, *294*, 418–431.
203. Schulze, J.; Houthoofd, W.; Uenk, J.; Vangestel, S.; Schierenberg, E. Plectus—A stepping stone in embryonic cell lineage evolution of nematodes. *Evodevo* **2012**, *3*, doi:10.1186/2041-9139-3-13.
204. Schulze, J.; Schierenberg, E. Evolution of embryonic development in nematodes. *Evodevo* **2011**, *2*, doi:10.1186/2041-9139-2-18.
205. Coutelis, J.B.; González-Morales, N.; Géminard, C.; Noselli, S. Diversity and convergence in the mechanisms establishing L/R asymmetry in metazoa. *EMBO Rep.* **2014**, *15*, 926–937.
206. Hozumi, S.; Maeda, R.; Taniguchi, K.; Kanai, M.; Shirakabe, S.; Sasamura, T.; Spéder, P.; Noselli, S.; Aigaki, T.; Murakami, R.; *et al.* An unconventional myosin in *Drosophila* reverses the default handedness in visceral organs. *Nature* **2006**, *440*, 798–802.
207. Spéder, P.; Adám, G.; Noselli, S. Type ID unconventional myosin controls left-right asymmetry in *Drosophila*. *Nature* **2006**, *440*, 803–807.

208. Géminard, C.; González-Morales, N.; Coutelis, J.B.; Noselli, S. The myosin ID pathway and left-right asymmetry in *Drosophila*. *Genesis* **2014**, *52*, 471–480.
209. Kim, S.V.; Flavell, R.A. Myosin I: From yeast to human. *Cell Mol. Life Sci.* **2008**, *65*, 2128–2137.
210. Pyrpassopoulos, S.; Feeser, E.; Mazerik, J.N.; Tyska, M.J.; Ostap, E.M. Membrane-bound Myo1c powers asymmetric motility of actin filaments. *Curr. Biol.* **2012**, *22*, 1688–1692.
211. Okumura, T.; Sasamura, T.; Inatomi, M.; Hozumi, S.; Nakamura, M.; Hatori, R.; Taniguchi, K.; Nakazawa, N.; Suzuki, E.; Maeda, R.; *et al.* Class I myosins have overlapping and specialized functions in left-right asymmetric development in *Drosophila*. *Genetics* **2015**, *199*, 1183–1199.
212. Petzoldt, A.G.; Coutelis, J.B.; Géminard, C.; Spéder, P.; Suzanne, M.; Cerezo, D.; Noselli, S. DE-Cadherin regulates unconventional Myosin ID and Myosin IC in *Drosophila* left-right asymmetry establishment. *Development* **2012**, *139*, 1874–1884.
213. Brembeck, F.H.; Rosário, M.; Birchmeier, W. Balancing cell adhesion and Wnt signaling, the key role of beta-catenin. *Curr. Opin. Genet. Dev.* **2006**, *16*, 51–59.
214. González-Morales, N.; Géminard, C.; Lebreton, G.; Cerezo, D.; Coutelis, J.-B.; Noselli, S. The atypical cadherin dachsous controls left-right asymmetry in *Drosophila*. *Dev. Cell* **2015**, *33*, 675–689.
215. Marcinkevicius, E.; Zallen, J.A. Regulation of cytoskeletal organization and junctional remodeling by the atypical cadherin Fat. *Development* **2013**, *140*, 433–443.
216. Hatori, R.; Ando, T.; Sasamura, T.; Nakazawa, N.; Nakamura, M.; Taniguchi, K.; Hozumi, S.; Kikuta, J.; Ishii, M.; Matsuno, K. Left-right asymmetry is formed in individual cells by intrinsic cell chirality. *Mech. Dev.* **2014**, *133*, 146–162.
217. Kuroda, J.; Nakamura, M.; Yoshida, M.; Yamamoto, H.; Maeda, T.; Taniguchi, K.; Nakazawa, N.; Hatori, R.; Ishio, A.; Ozaki, A.; *et al.* Canonical Wnt signaling in the visceral muscle is required for left-right asymmetric development of the *Drosophila* midgut. *Mech. Dev.* **2012**, *128*, 625–639.
218. Coutelis, J.B.; Géminard, C.; Spéder, P.; Suzanne, M.; Petzoldt, A.G.; Noselli, S. *Drosophila* left/right asymmetry establishment is controlled by the Hox gene abdominal-B. *Dev. Cell* **2013**, *24*, 89–97.
219. Haigo, S.L.; Bilder, D. Global tissue revolutions in a morphogenetic movement controlling elongation. *Science* **2011**, *331*, 1071–1074.
220. Viktorinová, I.; Dahmann, C. Microtubule polarity predicts direction of egg chamber rotation in *Drosophila*. *Curr. Biol.* **2013**, *23*, 1472–1477.
221. Cetera, M.; Ramirez-San Juan, G.R.; Oakes, P.W.; Lewellyn, L.; Fairchild, M.J.; Tanentzapf, G.; Gardel, M.L.; Horne-Badovinac, S. Epithelial rotation promotes the global alignment of contractile actin bundles during *Drosophila* egg chamber elongation. *Nat. Commun.* **2014**, *5*, doi:10.1038/ncomms6511.
222. Wang, H.; Lacoche, S.; Huang, L.; Xue, B.; Muthuswamy, S.K. Rotational motion during three-dimensional morphogenesis of mammary epithelial acini relates to laminin matrix assembly. *Proc. Natl. Acad. Sci. USA* **2013**, *110*, 163–168.
223. Thitamadee, S.; Tsuchihara, K.; Hashimoto, T. Microtubule basis for left-handed helical growth in *Arabidopsis*. *Nature* **2002**, *417*, 193–196.
224. Buschmann, H.; Fabri, C.O.; Hauptmann, M.; Hutzler, P.; Laux, T.; Lloyd, C.W.; Schäffner, A.R. Helical growth of the *Arabidopsis* mutant *tortifolia1* reveals a plant-specific microtubule-associated protein. *Curr. Biol.* **2004**, *14*, 1515–1521.

225. Lobikin, M.; Wang, G.; Xu, J.; Hsieh, Y.W.; Chuang, C.F.; Lemire, J.M.; Levin, M. Early, nonciliary role for microtubule proteins in left-right patterning is conserved across kingdoms. *Proc. Natl. Acad. Sci. USA* **2012**, *109*, 12586–12591.
226. Chang, C.; Hsieh, Y.W.; Lesch, B.J.; Bargmann, C.I.; Chuang, C.F. Microtubule-based localization of a synaptic calcium-signaling complex is required for left-right neuronal asymmetry in *C. elegans*. *Development* **2011**, *138*, 3509–3518.
227. Buschmann, H.; Hauptmann, M.; Niessing, D.; Lloyd, C.W.; Schäffner, A.R. Helical growth of the *Arabidopsis* mutant *tortifolia2* does not depend on cell division patterns but involves handed twisting of isolated cells. *Plant Cell* **2009**, *21*, 2090–2106.
228. Hoson, T.; Matsumoto, S.; Soga, K.; Wakabayashi, K. Cortical microtubules are responsible for gravity resistance in plants. *Plant Signal Behav.* **2010**, *5*, 752–754.
229. Oda, Y.; Fukuda, H. Initiation of cell wall pattern by a Rho- and microtubule-driven symmetry breaking. *Science* **2012**, *337*, 1333–1336.
230. Afzelius, B. A human syndrome caused by immotile cilia. *Science* **1976**, *193*, 317–319.
231. Wagner, M.K.; Yost, H.J. Left-right development: The roles of nodal cilia. *Curr. Biol.* **2000**, *10*, R149–R151.
232. Lee, J.D.; Anderson, K.V. Morphogenesis of the node and notochord: The cellular basis for the establishment and maintenance of left-right asymmetry in the mouse. *Dev. Dyn.* **2008**, *237*, 3464–3476.
233. Babu, D.; Roy, S. Left-right asymmetry: Cilia stir up new surprises in the node. *Open Biol.* **2013**, *3*, doi:10.1098/rsob.130052.
234. Komatsu, Y.; Mishina, Y. Establishment of left-right asymmetry in vertebrate development: The node in mouse embryos. *Cell Mol. Life Sci.* **2013**, *70*, 4659–4666.
235. Supp, D.M.; Witte, D.P.; Potter, S.S.; Brueckner, M. Mutation of an axonemal dynein affects left-right asymmetry in *inversus viscerum* mice. *Nature* **1997**, *389*, 963–966.
236. Nonaka, S.; Tanaka, Y.; Okada, Y.; Takeda, S.; Harada, A.; Kanai, Y.; Kido, M.; Hirokawa, N. Randomization of left-right asymmetry due to loss of nodal cilia generating leftward flow of extraembryonic fluid in mice lacking KIF3B motor protein. *Cell* **1998**, *95*, 829–837.
237. Okada, Y.; Nonaka, S.; Tanaka, Y.; Saijoh, Y.; Hamada, H.; Hirokawa, N. Abnormal nodal flow precedes situs inversus in *iv* and *inv* mice. *Mol. Cell* **1999**, *4*, 459–468.
238. Supp, D.M.; Brueckner, M.; Kuehn, M.R.; Witte, D.P.; Lowe, L.A.; McGrath, J.; Corrales, J.; Potter, S.S. Targeted deletion of the ATP binding domain of left-right dynein confirms its role in specifying development of left-right asymmetries. *Development* **1999**, *126*, 5495–5504.
239. Essner, J.J.; Amack, J.D.; Nyholm, M.K.; Harris, E.B.; Yost, H.J. Kupffer's vesicle is a ciliated organ of asymmetry in the zebrafish embryo that initiates left-right development of the brain, heart and gut. *Development* **2005**, *132*, 1247–1260.
240. Schweickert, A.; Weber, T.; Beyer, T.; Vick, P.; Bogusch, S.; Feistel, K.; Blum, M. Cilia-driven leftward flow determines laterality in *Xenopus*. *Curr. Biol.* **2007**, *17*, 60–66.
241. Nonaka, S.; Shiratori, H.; Saijoh, Y.; Hamada, H. Determination of left-right patterning of the mouse embryo by artificial nodal flow. *Nature* **2002**, *418*, 96–99.
242. Levin, M.; Johnson, R.L.; Sterna, C.D.; Kuehn, M.; Tabin, C. A molecular pathway determining left-right asymmetry in chick embryogenesis. *Cell* **1995**, *82*, 803–814.

243. Meno, C.; Saijoh, Y.; Fujii, H.; Ikeda, M.; Yokoyama, T.; Yokoyama, M.; Toyoda, Y.; Hamada, H. Left-right asymmetric expression of the TGF beta-family member lefty in mouse embryos. *Nature* **1996**, *381*, 151–155.
244. Collignon, J.; Varlet, I.; Robertson, E.J. Relationship between asymmetric nodal expression and the direction of embryonic turning. *Nature* **1996**, *381*, 155–158.
245. Lowe, L.A.; Supp, D.M.; Sampath, K.; Yokoyama, T.; Wright, C.V.E.; Potter, S.S.; Overbeek, P.; Kuehn, M.R. Conserved left-right asymmetry of nodal expression and alterations in murine *situs inversus*. *Nature* **1996**, *381*, 158–161.
246. Tanaka, Y.; Okada, Y.; Hirokawa, N. FGF-induced vesicular release of Sonic hedgehog and retinoic acid in leftward nodal flow is critical for left-right determination. *Nature* **2005**, *435*, 172–177.
247. Shinohara, K.; Kawasumi, A.; Takamatsu, A.; Yoshida, S.; Botilde, Y.; Motoyama, N.; Reith, W.; Durand, B.; Shiratori, H.; Hamada, H. Two rotating cilia in the node cavity are sufficient to break left-right symmetry in the mouse embryo. *Nat. Commun.* **2012**, *3*, 622.
248. McGrath, J.; Somlo, S.; Makova, S.; Tian, X.; Brueckner, M. Two populations of node monocilia initiate left-right asymmetry in the mouse. *Cell* **2003**, *114*, 61–73.
249. Noël, E.S.; Verhoeven, M.; Lagendijk, A.K.; Tessadori, F.; Smith, K.; Choorapoikayil, S.; Hertog, D.J.; Bakkers, J. A Nodal-independent and tissue-intrinsic mechanism controls heart-looping chirality. *Nat. Commun.* **2013**, *4*, doi:10.1038/ncomms3754.
250. Stephen, L.A.; Johnson, E.J.; Davis, G.M.; McTeir, L.; Pinkham, J.; Jaber, N.; Davey, M.G. The chicken left right organizer has nonmotile cilia which are lost in a stage-dependent manner in the *talpid³* ciliopathy. *Genesis* **2014**, *52*, 600–613.
251. Wang, G.; Manning, M.L.; Amack, J.D. Regional cell shape changes control form and function of Kupffer's vesicle in the zebrafish embryo. *Dev. Biol.* **2012**, *370*, 52–62.
252. Itasaki, N.; Nakamura, H.; Sumida, H.; Yasuda, M. Actin bundles on the right side in the caudal part of the heart tube play a role in dextro-looping in the embryonic chick heart. *Anat. Embryol.* **1991**, *183*, 29–39.
253. Blum, M.; Schweickert, A.; Vick, P.; Wright, C.V.; Danilchik, M.V. Symmetry breakage in the vertebrate embryo: When does it happen and how does it work? *Dev. Biol.* **2014**, *393*, 109–123.
254. Danilchik, M.V.; Brown, E.E.; Riegert, K. Intrinsic chiral properties of the *Xenopus* egg cortex: An early indicator of left-right asymmetry? *Development* **2006**, *133*, 4517–4526.
255. Bray, D.; White, J.G. Cortical flow in animal cells. *Science* **1988**, *239*, 883–888.
256. Lewis, W.H. The role of a superficial plasmagel layer in changes of form, locomotion and division of cells in tissue culture. *Arch. Exp. Zellforsch.* **1939**, *23*, 1–7.
257. Strome, S. Asymmetric movements of cytoplasmic components in *Caenorhabditis elegans* zygotes. *J. Embryol. Exp. Morphol.* **1986**, *97*, 15–29.
258. Hird, S.N.; White, J.G. Cortical and cytoplasmic flow polarity in early embryonic cells of *Caenorhabditis elegans*. *J. Cell Biol.* **1993**, *121*, 1343–1355.
259. Hird, S. Cortical actin movements during the first cell cycle of the *Caenorhabditis elegans* embryo. *J. Cell Sci.* **1996**, *109*, 525–533.
260. Goldstein, B.; Hird, S.N. Specification of the anteroposterior axis in *Caenorhabditis elegans*. *Development* **1996**, *122*, 1467–1474.

261. Sadler, P.L.; Shakes, D.C. Anucleate *Caenorhabditis elegans* sperm can crawl, fertilize oocytes and direct anterior-posterior polarization of the 1-cell embryo. *Development* **2000**, *127*, 355–366.
262. Nance, J.; Priess, J.R. Cell polarity and gastrulation in *C. elegans*. *Development* **2002**, *129*, 387–397.
263. Lee, J.Y.; Goldstein, B. Mechanisms of cell positioning during *C. elegans* gastrulation. *Development* **2003**, *130*, 307–320.
264. Nance, J.; Munro, E.M.; Priess, J.R. *C. elegans* PAR-3 and PAR-6 are required for apicobasal asymmetries associated with cell adhesion and gastrulation. *Development* **2003**, *130*, 5339–5350.
265. Lee, J.Y.; Marston, D.J.; Walston, T.; Hardin, J.; Halberstadt, A.; Goldstein, B. Wnt/frizzled signaling controls *C. elegans* gastrulation by activating actomyosin contractility. *Curr. Biol.* **2006**, *16*, 1986–1997.
266. Rohrschneider, M.R.; Nance, J. Polarity and cell fate specification in the control of *Caenorhabditis elegans* gastrulation. *Dev. Dyn.* **2009**, *238*, 789–796.
267. Roh-Johnson, M.; Shemer, G.; Higgins, C.D.; McClellan, J.H.; Werts, A.D.; Tulu, U.S.; Gao, L.; Betzig, E.; Kiehart, D.P.; Goldstein, B. Triggering a cell shape change by exploiting preexisting actomyosin contractions. *Science* **2012**, *335*, 1232–1235.
268. Wang, X.; Zhou, F.; Lv, S.; Yi, P.; Zhu, Z.; Yang, Y.; Feng, G.; Li, W.; Ou, G. Transmembrane protein MIG-13 links the Wnt signaling and Hox genes to the cell polarity in neuronal migration. *Proc. Natl. Acad. Sci. USA* **2013**, *110*, 11175–11180.
269. Witze, E.S.; Litman, E.S.; Argast, G.M.; Moon, R.T.; Ahn, N.G. Wnt5a control of cell polarity and directional movement by polarized redistribution of adhesion receptors. *Science* **2008**, *320*, 365–369.
270. Gon, H.; Fumoto, K.; Ku, Y.; Matsumoto, S.; Kikuchi, A. Wnt5a signaling promotes apical and basolateral polarization of single epithelial cells. *Mol. Biol. Cell* **2013**, *24*, 3764–3774.
271. Cui, C.; Chatterjee, B.; Lozito, T.P.; Zhang, Z.; Francis, R.J.; Yagi, H.; Swanhart, L.M.; Sanker, S.; Francis, D.; Yu, Q.; *et al.* Wdpcp, a PCP protein required for ciliogenesis, regulates directional cell migration and cell polarity by direct modulation of the actin cytoskeleton. *PLoS Biol.* **2013**, *11*, doi:10.1371/journal.pbio.1001720.
272. Dickinson, D.J.; Nelson, W.J.; Weis, W.I. A polarized epithelium organized by β - and α -catenin predates cadherin and metazoan origins. *Science* **2011**, *331*, 1336–1339.
273. St Johnston, D.; Ahringer, J. Cell polarity in eggs and epithelia: Parallels and diversity. *Cell* **2010**, *141*, 757–774.
274. Roth, S.; Lynch, J.A. Symmetry breaking during *Drosophila* oogenesis. *Cold Spring Harb. Perspect. Biol.* **2009**, *1*, doi:10.1101/cshperspect.a001891.
275. Doerflinger, H.; Benton, R.; Torres, I.L.; Zwart, M.F.; St Johnston, D. *Drosophila* anterior-posterior polarity requires actin-dependent PAR-1 recruitment to the oocyte posterior. *Curr. Biol.* **2006**, *16*, 1090–1095.
276. Leibfried, A.; Müller, S.; Ephrussi, A. A Cdc42-regulated actin cytoskeleton mediates *Drosophila* oocyte polarization. *Development* **2013**, *140*, 362–371.
277. Kiehart, D.P.; Lutz, M.S.; Chan, D.; Ketchum, A.S.; Laymon, R.A.; Nguyen, B.; Goldstein, L.S. Identification of the gene for fly non-muscle myosin heavy chain: *Drosophila* myosin heavy chains are encoded by a gene family. *EMBO J.* **1989**, *8*, 913–922.

278. Young, P.E.; Richman, A.M.; Ketchum, A.S.; Kiehart, D.P. Morphogenesis in *Drosophila* requires nonmuscle myosin heavy chain function. *Genes Dev.* **1993**, *7*, 29–41.
279. Blankenship, J.T.; Wieschaus, E. Two new roles for the *Drosophila* AP patterning system in early morphogenesis. *Development* **2001**, *128*, 5129–5138.
280. Zallen, J.A.; Wieschaus, E. Patterned gene expression directs bipolar planar polarity in *Drosophila*. *Dev. Cell* **2004**, *6*, 343–355.
281. Dawes-Hoang, R.E.; Parmar, K.M.; Christiansen, A.E.; Phelps, C.B.; Brand, A.H.; Wieschaus, E.F. Folded gastrulation, cell shape change and the control of myosin localization. *Development* **2005**, *132*, 4165–4178.
282. Bertet, C.; Sulak, L.; Lecuit, T. Myosin-dependent junction remodelling controls planar cell intercalation and axis elongation. *Nature* **2004**, *429*, 667–671.
283. Rauzi, M.; Verant, P.; Lecuit, T.; Lenne, P.F. Nature and anisotropy of cortical forces orienting *Drosophila* tissue morphogenesis. *Nat. Cell Biol.* **2008**, *10*, 1401–1410.
284. Fernandez-Gonzalez, R.; Simoes Sde, M.; Röper, J.C.; Eaton, S.; Zallen, J.A. Myosin II dynamics are regulated by tension in intercalating cells. *Dev. Cell* **2009**, *17*, 736–743.
285. Martin, A.C.; Kaschube, M.; Wieschaus, E.F. Pulsed contractions of an actin-myosin network drive apical constriction. *Nature* **2009**, *457*, 495–499.
286. Rauzi, M.; Lenne, P.F.; Lecuit, T. Planar polarized actomyosin contractile flows control epithelial junction remodelling. *Nature* **2010**, *468*, 1110–1114.
287. Simões Sde, M.; Mainieri, A.; Zallen, J.A. Rho GTPase and Shroom direct planar polarized actomyosin contractility during convergent extension. *J. Cell Biol.* **2014**, *204*, 575–589.
288. Kasza, K.E.; Farrell, D.L.; Zallen, J.A. Spatiotemporal control of epithelial remodeling by regulated myosin phosphorylation. *Proc. Natl. Acad. Sci. USA* **2014**, *111*, 11732–11737.
289. He, B.; Dubrovinski, K.; Polyakov, O.; Wieschaus, E. Apical constriction drives tissue-scale hydrodynamic flow to mediate cell elongation. *Nature* **2014**, *508*, 392–396.
290. Munjal, A.; Philippe, J.M.; Munro, E.; Lecuit, T. A self-organized biomechanical network drives shape changes during tissue morphogenesis. *Nature* **2015**, doi:10.1038/nature14603.
291. Behrndt, M.; Salbreux, G.; Campinho, P.; Hauschild, R.; Oswald, F.; Roensch, J.; Grill, S.W.; Heisenberg, C.P. Forces driving epithelial spreading in zebrafish gastrulation. *Science* **2012**, *338*, 257–260.
292. Yi, K.; Rubinstein, B.; Li, R. Symmetry breaking and polarity establishment during mouse oocyte maturation. *Philos. Trans. R. Soc. Lond. B Biol. Sci.* **2013**, *368*, doi:10.1098/rstb.2013.0002.
293. Lepage, S.E.; Bruce, A.E.E. Zebrafish epiboly: Mechanics and mechanisms. *Int. J. Dev. Biol.* **2010**, *54*, 1213–1228.
294. Lucas, E.P.; Khanal, I.; Gaspar, P.; Fletcher, G.C.; Polesello, C.; Tapon, N.; Thompson, B.J. The Hippo pathway polarizes the actin cytoskeleton during collective migration of *Drosophila* border cells. *J. Cell Biol.* **2013**, *201*, 875–885.
295. Goldstein, B. Cell contacts orient some cell division axes in the *Caenorhabditis elegans* embryo. *J. Cell Biol.* **1995**, *129*, 1071–1080.
296. Thorpe, C.J.; Schlesinger, A.; Carter, J.C.; Bowerman, B. Wnt signaling polarizes an early *C. elegans* blastomere to distinguish endoderm from mesoderm. *Cell* **1997**, *90*, 695–705.

297. Schlesinger, A.; Shelton, C.A.; Maloof, J.N.; Meneghini, M.; Bowerman, B. Wnt pathway components orient a mitotic spindle in the early *Caenorhabditis elegans* embryo without requiring gene transcription in the responding cell. *Genes Dev.* **1999**, *13*, 2028–2038.
298. Bei, Y.; Hogan, J.; Berkowitz, L.A.; Soto, M.; Rocheleau, C.E.; Pang, K.M.; Collins, J.; Mello, C.C. SRC-1 and Wnt signaling act together to specify endoderm and to control cleavage orientation in early *C. elegans* embryos. *Dev. Cell* **2002**, *3*, 113–125.
299. Goldstein, B.; Takeshita, H.; Mizumoto, K.; Sawa, H. Wnt signals can function as positional cues in establishing cell polarity. *Dev. Cell* **2006**, *10*, 391–396.
300. Arata, Y.; Lee, J.Y.; Goldstein, B.; Sawa, H. Extracellular control of PAR protein localization during asymmetric cell division in the *C. elegans* embryo. *Development* **2010**, *137*, 3337–3345.
301. Habib, S.J.; Chen, B.C.; Tsai, F.C.; Anastassiadis, K.; Meyer, T.; Betzig, E.; Nusse, R. A localized Wnt signal orients asymmetric stem cell division *in vitro*. *Science* **2013**, *339*, 1445–1448.
302. Sugioka, K.; Mizumoto, K.; Sawa, H. Wnt regulates spindle asymmetry to generate asymmetric nuclear β -catenin in *C. elegans*. *Cell* **2011**, *146*, 942–954.
303. Knoblich, J.A. Asymmetric cell division: Recent developments and their implications for tumour biology. *Nat. Rev. Mol. Cell Biol.* **2010**, *11*, 849–860.
304. Pelletier, L.; Yamashita, Y.M. Centrosome asymmetry and inheritance during animal development. *Curr. Opin. Cell Biol.* **2012**, *24*, 541–546.
305. Lu, M.S.; Johnston, C.A. Molecular pathways regulating mitotic spindle orientation in animal cells. *Development* **2013**, *140*, 1843–1856.
306. O'Donnell, L.; O'Bryan, M.K. Microtubules and spermatogenesis. *Semin. Cell Dev. Biol.* **2014**, *30*, 45–54.
307. Segalen, M.; Bellaïche, Y. Cell division orientation and planar cell polarity pathways. *Semin. Cell Dev. Biol.* **2009**, *20*, 972–977.
308. Goodrich, L.V.; Strutt, D. Principles of planar polarity in animal development. *Development* **2011**, *138*, 1877–1892.
309. Matis, M.; Axelrod, J.D. Regulation of PCP by the Fat signaling pathway. *Genes Dev.* **2013**, *27*, 2207–2220.
310. Guirao, B.; Meunier, A.; Mortaud, S.; Aguilar, A.; Corsi, J.M.; Strehl, L.; Hirota, Y.; Desoeuvre, A.; Boutin, C.; Han, Y.G.; *et al.* Coupling between hydrodynamic forces and planar cell polarity orients mammalian motile cilia. *Nat. Cell Biol.* **2010**, *12*, 341–350.